UPPSALA
UNIVERSITET

Digital Comprehensive Summaries of Uppsala Dissertations from the Faculty of Science and Technology 731

By Means of Beams

Laser Patterning and Stability in CIGS Thin Film Photovoltaics

PER-OSKAR WESTIN

ACTA
UNIVERSITATIS
UPSALIENSIS
UPPSALA
2011

ISSN 1651-6214
ISBN 978-91-554-7988-6
urn:nbn:se:uu:diva-143154

Dissertation presented at Uppsala University to be publicly examined in Å4001, Ångströmlaboratoriet, Lägerhyddsvägen 1, Uppsala, Friday, March 4, 2011 at 09:30 for the degree of Doctor of Philosophy. The examination will be conducted in English.

Abstract
Westin, P-O. 2011. By Means of Beams. Laser Patterning and Stability in CIGS Thin Film Photovoltaics. Acta Universitatis Upsaliensis. *Digital Comprehensive Summaries of Uppsala Dissertations from the Faculty of Science and Technology* 731. 98 pp. Uppsala. ISBN 978-91-554-7988-6.

Solar irradiation is a vast and plentiful source of energy. The use of photovoltaic (PV) devices to convert solar energy directly to electrical energy is an elegant way of sustainable power generation which can be distributed or in large PV plants based on the need. *Solar cells* are the small building blocks of photovoltaics and when connected together they form PV *modules*. Thin film solar cells require significantly less energy and raw materials to be produced, as compared to the dominant Si wafer technologies. CIGS thin film solar cells are considered to be the most promising thin film alternative due to its proven high efficiency.

Most thin film PV modules utilise monolithic integration, whereby thin film patterning steps are included between film deposition steps, to create interconnection of individual cells within the layered structure. The state of the art is that CIGS thin film modules are made using one laser patterning step (P1) and two mechanical patterning steps (P2 and P3). Here we present work which successfully demonstrates the replacement of mechanical patterning by laser patterning methods. The use of laser ablation promises such advantages as increased active cell area and reduced maintenance and downtime required for regular replacement of mechanical tools.

The laser tool can also be used to transform CIGS into a conducting compound along a patterned line. We have shown that this process can be performed after all semiconductor layers are deposited using a technique we call *laser micro-welding*. By performing patterning at the end of the process flow P2 and P3 patterning could be performed simultaneously. Such solutions will further reduce manufacturing times and may offer increased control of semiconductor interfaces.

While showing promising performance on par with reference processes there are still open questions of importance for these novel techniques, particularly that of long term stability. Thin film modules are inherently sensitive to moisture and require reliable encapsulation. Before the techniques introduced here can be seen industrially they must have achieved proven stability. In this work we present a proof of existence of stable micro-welded interconnections.

Keywords: Laser patterning, laser ablation, laser micro-welding, stability, Cu(InGa)Se2, CIGS, thin film solar cells, thin film photovoltaics, module technology, solar energy

Per-Oskar Westin, Department of Engineering Sciences, Solid State Electronics, Box 534, Uppsala University, SE-75121 Uppsala, Sweden.

ISSN 1651-6214
ISBN 978-91-554-7988-6
urn:nbn:se:uu:diva-143154 (http://urn.kb.se/resolve?urn=urn:nbn:se:uu:diva-143154)

"We had good reasons for what we were doing.
One was that it seemed entirely possible."
- Scott Carrier

I would like to dedicate this work to those who believed in me
even though they had no idea what I was doing.
And to those who knew very well what I was doing
and still believed in me.

List of Papers

This thesis is based on the following papers, which are referred to in the text by their Roman numerals.

I P-O. Westin, S. C. Schmidt, M. Hüske and M. Edoff. (2009) Influence of spacial and temporal laser beam characteristics on thin-film ablation. Proceedings of the 24th European Photovoltaic Solar Energy Conference, München.

II P-O. Westin, P. Neretnieks and M. Edoff. (2006) Damp heat degradation of CIGS-based PV modules. Proceedings of the 21st European Photovoltaic Solar Energy Conference, Dresden

III P-O. Westin, U. Zimmermann and M. Edoff. (2008) Laser patterning of P2 interconnect via in thin-film CIGS PV modules. Solar Energy Materials & Solar Cells 92 pp.1230

IV P-O. Westin, U. Zimmermann, L. Stolt and M. Edoff. (2009) Reverse-bias damage in CIGS modules. Proceedings of the 24th European Photovoltaic Solar Energy Conference, München.

V P-O. Westin, U. Zimmermann, M. Ruth and M. Edoff. (2011) Next generation interconnective laser patterning of CIGS thin film modules. Solar Energy Materials & Solar Cells. (In Press.)

VI P-O. Westin, T. Wätjen and Edoff, M. Microanalysis of laser micro-welded interconnections in CIGS PV modules. (Manuscript)

VII P-O. Westin and M. Edoff. (2008) Materials analysis of laser treated CIGS. Proceedings of the 23rd European Photovoltaic Solar Energy Conference, Valencia

Related Papers

The following papers are the outcome of research work done outside the scope of this thesis.

B. R. Olaisen, S. Woldegiorgis, P-O. Westin, M. Edoff, L. Stolt, A. Holt and E. Stensrud Marstein. (2005) CIGS mini-modules with screen printed front contacts. Proceedings of 15th International Photovoltaic Science and Engineering Conference (PVSEC-15) : October 10 - 15, 2005, Shanghai.

M. Edoff, N. Viard, T. Wätjen, S. Schleussner, P-O. Westin and K. Leifer. (2009) Sputtering of highly adhesive Mo back contact layers for Cu(In,Ga)Se_2 solar cells. Proceedings of the 24th European Photovoltaic Solar Energy Conference, München.

Reprints were made with permission from the publishers.

Contents

Abbreviations and Symbols used

α	Absorption coefficient
χ	Thermal diffusivity
η	Conversion efficiency
λ	Wavelength
τ_{las}	Laser pulse duration
d_{th}	Heat diffusion distance
$A(\lambda)$	Absorptivity
AC	Alternating current
a-Si	Amorphous silicon
CdTe	Cadmium telluride
CIGS	Copper-indium-gallium-diselenide
CSG	Crystalline silicon on glass
DC	Direct current
DH	Damp heat
E_c	Conduction band edge
E_g	Band gap
E_v	Valence band edge
EDS or EDX	Energy dispersive x-ray spectroscopy
eV	Electron volt
EVA	Ethylene vinyl acetate
FF	Fill factor
FTO	Fluorine doped tin oxide
I_{mp}	Current at maximum power
I_{sc}	Short circuit current
IR	Infrared
ITO	Indium tin oxide
ITS	Interconnect test structure
I-V	Current-Voltage
i-ZnO	Undoped (intrinsic) zinc oxide

LLC	Layered laser crystallisation
PV	Photovoltaic(s)
R_{sh}	Shunt resistance
R_c	Contact resistance
R_s	Series resistance
$R(\lambda)$	Reflectivity
RF	Radio frequency
RH	Relative Humidity
SEM	Scanning electron microscope
$T(\lambda)$	Transmissivity
TCO	Transparent conductive oxide
TEM	Transmission electron microscopy
UV	Ultraviolet
V_{mp}	Voltage at maximum power
V_{oc}	Open circuit voltage
XRD	X-ray diffractometry
XRF	X-ray fluorescense spectroscopy
YAG	Yttrium aluminium garnet
YVO_4	Yttrium vanadate
ZnO:Al	Aluminium doped zinc oxide

1. Introduction

1.1 Solar energy

It is a clear, bright day. In the shower of photons raining down from a cloudless sky we find an instinctive truth: that solar energy is a benefactor and an ever present support. Even on rainy, cloudy days or in the midst of night we find reassurance - at least once our cognitive development passes a certain point - in the fact that the sun will shine upon us once again. Without a doubt. What our sensitive skin and intuitive mind does not confer with any detail is the vastness of this realisation. Energy that is produced by the fusion reactions inside the our nearest star spreads in all directions and only a minuscule portion hits the earth. Even still, some 87'000 TW [1] is constantly available on the illuminated half sphere facing the sun. Every hour, every day. This number dwarfs the world consumption of energy and two hours worth of sunshine is more that what is needed to sustain our current civilisation for over a year [2].

Solar energy is distributed over a range of wavelengths, or photon energies, each having a specific intensity as shown in Figure 1.1, from the high energy ultraviolet (UV) radiation to low energy infrared (IR) radiation. There is a narrow range of energies that our eyes are sensitive to, more specifically 400 - 750 nm within which we experience the rainbow of colours from deep purple to red.

1.2 Electricity

Energy is a most essential commodity, one might say the strongest driver of development and growth of our society. The more energy available to us, the more we prosper and the more comfortable we manage to make our lives. Today few - if any - forms of energy permeate our lives more completely than does electricity. Electrical appliances are scattered around our homes, taking care of our dirty clothes, dirty dishes and clean entertainment. In most of the developed world it is rare to come across an individual that does not carry around at least one electronic device for communication or recreation. Uniquely transformable and scalable, electrical energy is the highest quality form of energy in terms of versatility, cleanness and shear power. It can provide light, sound, power tooling or even transport when fed into the proper devices. To combine the availability and vast quantity of solar energy with the

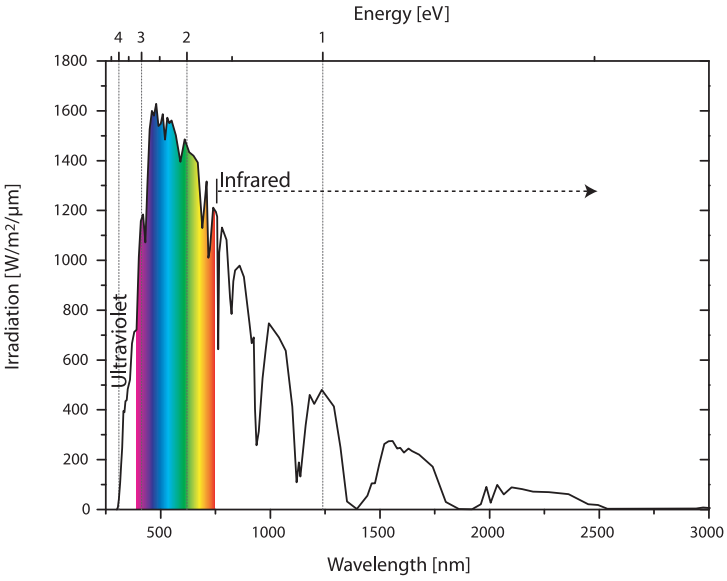

Figure 1.1: Solar energy spectrum of from ultraviolet to short wavelength infrared. The infrared region extends all the way to 1 mm wavelengths. The visible wavelengths are represented by the coloured portions of the spectrum.

elegance and versatility of electricity is an awesome dream. And the dream has a name - Photovoltaics.

1.3 Photovoltaic electricity generation

Photovoltaics, or PV for short, is the term used to describe electricity generation directly from light. A photovoltaic device, a solar cell, placed in the sun will operate in some ways like a battery. By connecting a circuit between its two terminals (+) and (-) a current will flow (provided that the cell is under illumination). The potential electrical energy driving this flow is given by the nature of the device and the flow of electrons that is generated can be utilized in any matched electrical load. For an illustrative example, Figure 1.2. shows a solar energy driven irrigation system. A small, mobile array of PV panels connected to a water pump delivers irrigation to a field when the sun shines. Of course, most uses of PV generated electricity are far more complex and involve additional electronics to keep the panel working at its maximum power and to perform inversion from the generated direct current (DC) to alternating current (AC) for grid connection. This thesis will not further consider PV as an installed power generator but will focus on some technological challenges involved in manufacturing thin film PV panels with high efficiencies at low cost. To begin, we will look a little more closely on what a solar cell is.

Figure 1.2: A simple photovoltaic system where a small mobile array of panels drives a water pump for irrigation. Image courtesy of Missouri Natural Resources Conservation Service (http://www.mo.nrcs.usda.gov/)

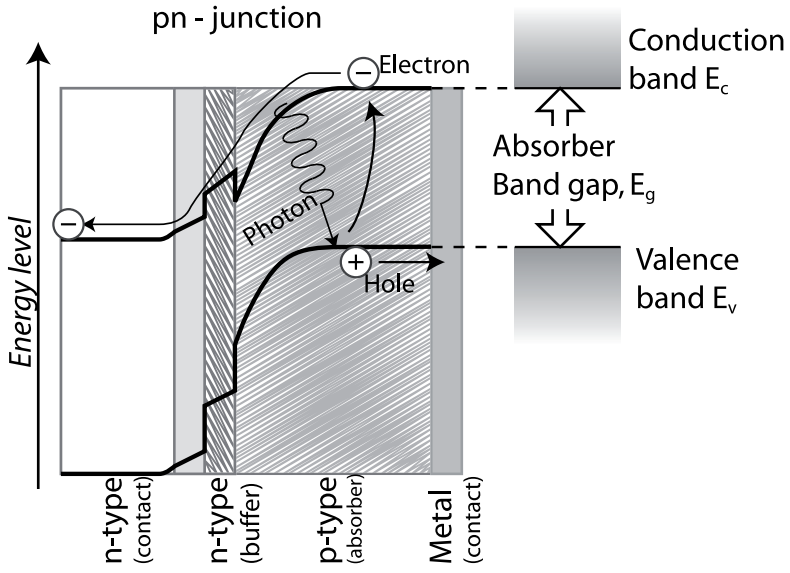

Figure 1.3: Band structure in a thin film solar cell showing the gap between the valence band and the conduction band. In order for absorption to occur, photon energy must exceed this energy gap. The energy difference across the pn-junction gives a solar cell its potential energy.

1.3.1 The solid state solar cell

The core of photovoltaics lies in transferring the photon energy in (sun-) light to electrons in a way that makes it possible to extract electrical energy. In solid materials the atomic structure will determine the "allowed" and "forbidden" energetic states of its electrons. For detailed explanation of how I will refer to any textbook on Solid State Physics, e.g. [3]. Depending on the atomic arrangement each solid will have an equilibrium energy level for its electrons called the *Fermi level*, E_F. In metals the equilibrium is in a range of energies that are allowed, leaving the electrons free to move around resulting in their electrical conductivity. In semiconductors and isolators however the equilibrium level is at an energy level that is forbidden. Below is a range of allowed energies called the *valence band*, whose top energy level is denoted E_v. Above the range of forbidden energies is another range of allowed energies. The top range is called the *conduction band* whose lowest energy is denoted E_c. The gap between the valence band top and conduction band bottom is called the *band gap*, E_g. If electrons can bridge this gap from the valence band to the conduction band, conductivity is introduced into the material, both due to the excited electrons and the *electron holes* they leave behind in the valence band who act like positively charged carriers. Holes that move in the opposite direction of electrons contribute to the same current flow. Since a large part of the energy in sunlight is between 1-4 eV, photovoltaic absorbers tend to have a band gap somewhere between 1-2 eV which allows utilisation of as much energy as possible.

We have energetic levels in sunlight and energetic levels in solid materials, now we are two thirds of the way there. What is lacking is the reason for the electronic driving force. If two semiconductor materials with different equilibrium levels - or a single material that has regions of different equilibrium levels - are put together, their energetic levels will not line up. Instead, the energy bands will realign to line up the equilibrium level. This will form a so-called *pn-junction* (see Figure 1.3), where the "p" and "n" regions differ in the type of free carriers. On the n-side of the junction, there is an excess of electrons in the conduction band. On the p-side of the junction there is and excess of free electron holes in the valence band. The difference in carrier concentrations is spontaneously compensated by a diffusion flow of carriers, a *diffusion current*. As more and more electrons cross the junction, a charge imbalance is built up with the p-side becoming negatively charged and the n-side positively charged. This builds an electric field across the junction between the materials, analogous to a water fall. Electrons near the junction will flow from higher energies to lower, crossing the junction (see Figure 1.3) in an oppositely directed current, the *drift current*. In equilibrium, the diffusion and drift currents will be equal and opposite and no current will pass through the cell.

This is where the photons come in handy. Every photon with an energy higher than the absorber band gap can potentially excite, or lift, an electron

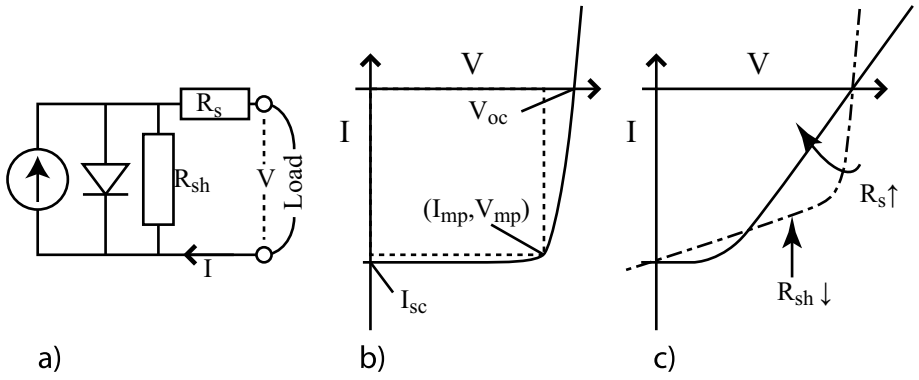

Figure 1.4: a) Equivalent circuit of a solar cell and b) ideal *I-V* curve showing the maximum power point. c) Effects on the I-V curve of increased series resistance or decreased shunt resistance.

from the valence band to the conduction band, replenishing the supply of electrons on the p-side. Current can be extracted from the solar cell by completing an external circuit between the p-side contact and n-side contact. The driving force is given by the potential energy difference across the junction and current will flow as long as new electrons are being excited in the absorber.

1.3.2 Equivalent circuit and I-V curve

A solar cell can be represented by an equivalent circuit that describes its function. This is explained thoroughly in e.g.[4]. The equivalent circuit consists of a current source representing the light generated current, a diode and internal series and shunt resistances as shown in Figure 1.4a. Depending on the external load the current and voltage output output of a solar cell will change. At zero load - a short circuit between terminals - a maximum current will flow in the circuit. It is termed the *short circuit current* I_{sc}. As the load is increased, an external voltage drop is introduced and the cell will change its operating point. With increased voltage across the terminals of the cell, current will start to flow through the shunt which is ideally very resistive. Eventually, the diode will become much more conductive and at one point all light generated current will pass through the diode, with zero current in the external circuit. This point is the *open circuit voltage*, V_{oc}. The highest power output of a solar cell is reached when the product

$$P = I(V) \cdot V \qquad [W] \tag{1.1}$$

reaches its maximum value (Figure 1.4b):

$$P_{max} = I_{mp}(V) \cdot V_{mp} \qquad [W] \tag{1.2}$$

The "squareness" of the described *I-V* curve gives an idea of the functionality of the cell and a measure of this is the *fill factor*. The fill factor is defined as

$$FF = 100 \cdot \frac{I_{mp} \cdot V_{mp}}{I_{sc} \cdot V_{oc}} \qquad [\%] \tag{1.3}$$

Increased resistances in series will pivot the curve at V_{oc}, and a decreased shunt resistance causes a leakage current in the cell. These effects are illustrated in 1.4 c). Both will lower the fill factor of the cell. Having defined P_{max} we can now state the efficiency of a solar cell. It is the ratio of P_{max} to total incident power on the solar cell:

$$\eta = 100 \cdot \frac{P_{max}}{P_{total}} \qquad [\%] \tag{1.4}$$

1.3.3 Silicon wafer solar cells

The most developed and most commonly used material for making solar cells is silicon. Pure silicon is extracted from sand, which is mostly quartz (SiO_2), that has been refined and crystallised. Refining silicon is a very energy intensive process, essentially since it requires high temperatures to melt and purify the silicon [5]. A typical silicon solar cell is made from thinly cut wafers whose thickness is in the order of 150 μm and that measure some 10-15 cm across. *Doping*, very small amounts of other elements introduced in the Si crystal, is what creates the p-type and n-type regions in the cell. To extract current, metal contacts are added on top and bottom of the cell, see Figure 1.5. While the 150 μm that are required for complete absorption of all wavelengths of light may seem thin - a human hair measures somewhere between 20-200 μm in diameter - thin film solar cells go even further, as we shall see.

1.3.4 Thin film solar cells

Thin film solar cells perform the same elegant magic of transforming rays of light into powerful ranks of electrons ready to do our bidding. What is more

Table 1.1: *Best cell and module efficiencies for the three most common thin film PV materials.*

Thin film technology	CIGS	CdTe	a-Si
Best Cell	19.4 %	16.7 %	10.1 %
Best large area module	13.8%	10.9 %	8.2 %
	Data cited from [6]		

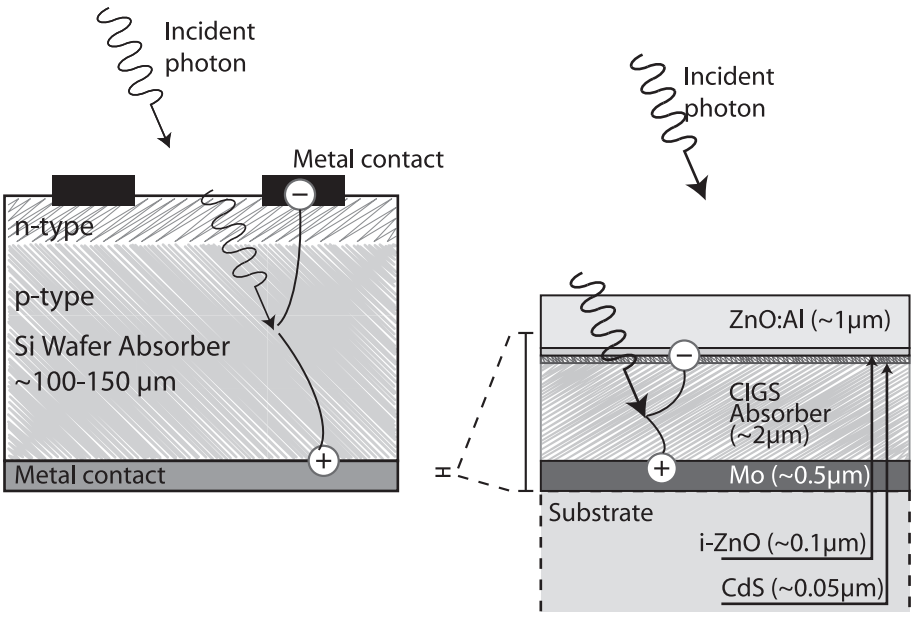

Figure 1.5: Photonic absorption in solar cells lead to charge separation which can be extracted as current. The Si wafer solar cell is ≈100X thicker than thin film solar cells.

impressive, they do this requiring only a fraction of the material and energy as compared to silicon wafer cells. Typical thicknesses are 2-10 μm for the entire solar cell. This is possible due to superior absorption properties of the thin film absorber materials [7]. Of course, a solar absorber material that is only a few μm thick requires a stable mechanical support, a carrier substrate onto which the thin films can be deposited. Thin film solar cells consist of an absorber material which, together with a buffer material to create the pn-junction, is sandwiched between two contact materials, see Figure 1.3. There are three main absorber materials being developed and commercialized today: *amorphous silicon* [1] (a-Si), *cadmium telluride* (CdTe) and *copper indium gallium diselenide* (CIGS). CIGS is the material that has shown the biggest promise in terms of efficiency (Table 1.1), while CdTe is the current champion in terms of low manufacturing costs. Since one side of the cell faces the sunlight, and radiation must pass through to reach the absorber, the topmost contact must be transparent for the relevant wavelengths. Commonly used materials include aluminium doped zinc oxide (ZnO:Al), indium tin oxide (ITO) and fluorine doped tin oxide (FTO). The bottom contact does not need to transmit radiation. On the contrary, it may be beneficial if the rear contact is reflecting, particularly if this reflectivity is in a range of wavelengths that the cell ab-

[1]There is actually a diverse family of derivative absorbers which I will refer to as simply a-Si since for the purpose of this thesis we are not obligated to differentiate them further

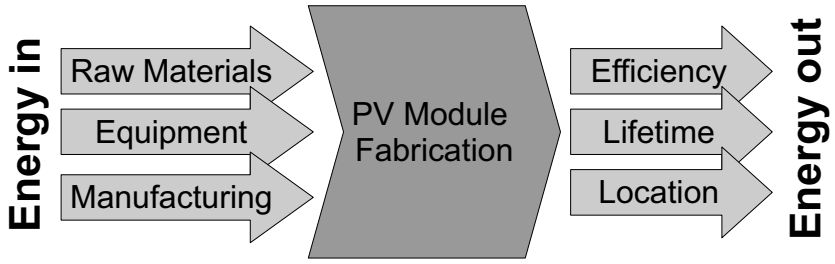

Figure 1.6: A simple flowchart to describe the main economics of photovoltaic module manufacturing. The more output and the less input the better. Combining efficiency, lifetime and irradiation at the installed location gives the energy output of the module.

sorbs less well. Common materials used in back contacts are molybdenum (Mo), Aluminium (Al) or silver (Ag). Figure 1.5 shows the layer stack used in most CIGS thin film solar cells - glass/Mo/CIGS/CdS/i-ZnO/ZnO:Al - along with typical thicknesses [8].

1.4 Thin film advantages

There is much to gain from thin film technology. Consider the chart in Figure 1.6. Using this simplified view allows us to reason briefly around the utility of PV and the advantages of thin films. As a source of power, PV must have a net gain in energy, i.e. $\text{Energy}_{Out} > \text{Energy}_{In}$, noting that Energy_{Out} is a product of module Efficiency and available sunlight (Location) for the duration of its Lifetime. This enables us to define *Energy Payback Time* (EPBT), a metric used when making life-cycle assessments for photovoltaic modules. It compares the total amount of energy used in manufacturing and installing a module with the energy returned after it is installed. EPBT is the time needed for a module to "regenerate" the invested, i.e. when $\text{Energy}_{Out} = \text{Energy}_{In}$. Calculations of EPBT are based on the efficiency of the panel and geographical data describing solar irradiance. EPBT is therefore dependent on the location where the module is installed. Investigations have repeatedly shown that modules based on thin film technology return the invested energy faster than modules made with crystalline wafers, independent of location. A 2006 estimate puts the EPBT of a CIGS module to just over 1 year and that of a multicrystalline Si module to just under 2 years in a southern Europe location [9]. This is primarily due to less energy used in manufacturing thin film modules. More

recent studies focused on CdTe showed that thin film technologies reduce the amount of all emissions and heavy metals released, including Cd [10]. It has also been noted that the greenhouse gas emissions of PV are related to the energy mix used in manufacturing. As the total electricity generation becomes less intense in emissions, the PV advantage will increase [5].

As a commercial product, it is required that there is an economic benefit of installing PV power generation. The cost of producing PV modules is essentially determined by the same factors as the energy input, with the addition of manpower costs. The economic return is, simplified, a function of the module efficiency, the geographic location, module lifetime *and* the price of electricity during its lifetime. The electricity price to consider will be different for an end-user and a large-scale electricity producer. Since the cost of electricity production is always lower than the price paid by end-users, generally speaking they are consequently the first to benefit from installing solar power. In a sense, the profit margin will be on the consumer side. This is of course a very simplified view and does not account for the benefits and cost reductions by large scale investments nor added costs that may apply in terms of certification, licenses etc. What is undisputable however is that the price of fossil fuels for electricity generation continues to rise [11] while the cost of PV will continue to decline [12, 13].

By using less material and less energy in manufacturing thin film PV inherently reduces the cost of PV manufacturing. Depending on the absorber material used, power output will be governed by its electronic properties and by the successful scaling of deposition technologies. Current world records for different absorber materials are given in Table 1.1 showing that CIGS is the most efficient thin film material and is therefore considered the most promising. Power output can also be increased by technological improvements, such as reduced area loss in patterning. For a comprehensive review on the industrial development and economical aspects of CIGS please refer to [12].

1.5 Industrial PhD project

Before going into the scientific part of the thesis I will also note that the bulk of this work has been done as a graduate industry project with the support and involvement of Solibro Research AB. Additional work was undertaken in close collaboration between the university research group, Ångström Solar Center, and Solibro but with the chief financial support of the Swedish Energy Agency. During this time Solibro has grown from a spin-off demonstration of CIGS upscaling to a commercial manufacturer under the Q-cells umbrella with 2 factories in operation in Bitterfeld-Wolfen (Germany), a nominal yearly output of 135 MW and a 14.2 % world record efficiency[2] for full-sized mono-

[2]All efficiencies reported in this work are aperture area efficiencies. The total area efficiency (including edges and frame) of the record module is 13 %.

lithically integrated CIGS modules achieved in the production line [14]. The research group in Sweden has become a Research and Development center with a complete line of manufacturing equipment and the goal of advancing CIGS deployment by providing next generation solutions along with strong support to the production facilities in Germany.

1.6 Aim of thesis

The aim of this thesis is to illuminate and discuss what can be gained from using laser processing in CIGS thin film PV module manufacturing. We will also consider lifetime and stability issues that concern CIGS modules as it is relevant to commercial deployment on a scale that will impact electricity generation on a global scale. In each of the coming chapters we will focus on the challenge of integrating multiple cells into large modules (Chapter 2); the laser tool and its characteristics when used for material processing (Chapter 3); how lasers are used - or more importantly how they *can* be used - to improve CIGS PV manufacturing (Chapter 4); and finally encapsulation and stability as it applies to CIGS modules (Chapter 5).

2. Thin film photovoltaic technology

2.1 Integration - cells to modules

As was explained in the introduction, solar cells are devices that generate electricity from light. Cells of crystalline Si have been limited in size by the methods of wafer preparation as well as by increased difficulties in handling larger and thinner wafers. This is not the case for thin film solar cells. One of the main requirements on the deposition methods selected for thin film solar module manufacturing is the ability to cover large areas with uniform material. However, one will still not find thin film solar cells of m^2 sizes. Instead, large modules consist of cells that are connected in series. Some manufacturers choose to deposit thin film cells on individual substrates that are subsequently assembled and interconnected either analogous to Si wafers, with metal grids and soldered contacts [15, 16], or in other ways, for example shingling of cell strips [17, 18]. This introduces additional steps in manufacturing such as handling, sorting, grid deposition, interconnection tabbing and soldering. The addition of a metal grid also increases area loss, shading and the risk of front-to-back shunting of cells, reducing performance and long term stability[19]. We refer to *thin film modules* only meaning modules that are in their entirety assembled using sequential thin film deposition and patterning on a single large area substrate, forming the elongated cell strips which lend them the characteristic pin-stripe appearance (as can be seen on the thesis cover).

2.2 Thin film PV modules

First, let us consider the basic characteristics of a solar cell. Output voltage is a function of the built-in voltage of the specific pn-junction and (ideally) independent on cell size. Generated current however depends linearly on the area of the solar cell. This becomes problematic as one makes the cell larger, since the junction voltage of the solar cell must drive the generated current through the contact layers to the edge of the cell before any current can be extracted. While a typical lab cell measures 0.5-1 cm^2 and the current is collected by a distributed grid, full size solar panels typically measure 1.2 x 0.6 m^2. A single solar cell of this size would generate around 150 A current with only 0.5 V bias in the maximum power point. Such a large current would incur high resistive losses and the voltage would not suffice even to drive the current through

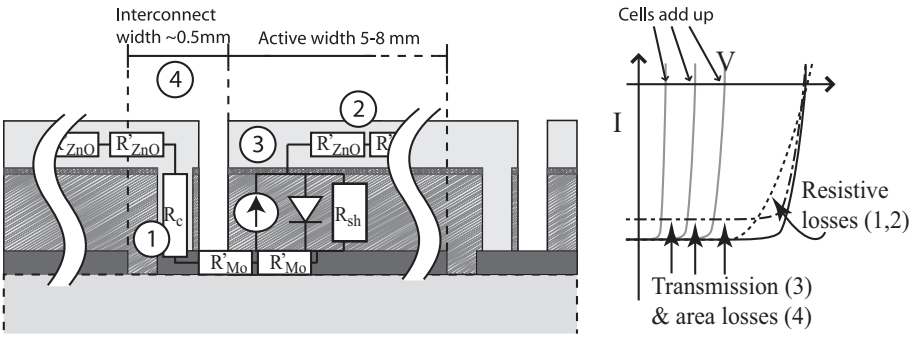

Figure 2.1: Cells connected in series make up a module. Losses include interconnect resistance (1), TCO resistance (2), increased TCO absorption (3) and area loss due to interconnection (4). Resistive losses reduce the fill factor (dotted line) in modules while absorption and area losses reduce current generation and fill factor (dash-dot).

the top contact layer to the edges. By separating cells into longs strips, where current passes only across the narrow width - 5-8 mm - of the cell, current is limited and resistive losses are reduced. The voltage of all cells is connected in series and adds up across the module width so that module output is high voltage and low current (see Figure 2.1).

We can now reconsider the information in Table 1.1. The table shows a wide gap between cell and module efficiencies. We can identify four inevitable contributors to this gap. (1) Separating the module into cells connected in series adds a contact resistance which increases resistive losses. (2) The cell width in a module is larger than the equivalent distance in a lab cell with a metal grid to collect the current. This increases the current density in the TCO layer and therefore the voltage drop incurred by resistive losses. This effect is countered by depositing thicker - and therefore less resistive - TCO layers in modules than what is used in a gridded lab cell. Consequently the thicker TCO layer introduces (3) more absorption in the window and less photons available for current generation in the absorber. Yet another current loss is incurred by the (4) surface area occupied by the interconnection of cells. Typically this is in the range of 5-10 % of the aperture area, a significant loss. Loss mechanisms (1) and (2) increase the series resistance which, as was illustrated in Figure 1.4, reduces the fill factor of modules. Absorption (3) and area (4) losses will primarily lower the current generated in a module but the upward shift of the I-V curve also has a reducing effect on the fill factor.

To this one must add losses that are due to issues of process homogeneity across the large area substrates. Since the module current crosses each individual cell, whichever cell generates the least current will be limiting for module output. With all cells working together, it is not possible to find the maximum power point for each cell. Instead, maximum output of a module is reached when the best compromise between cells is reached. Put together, all these

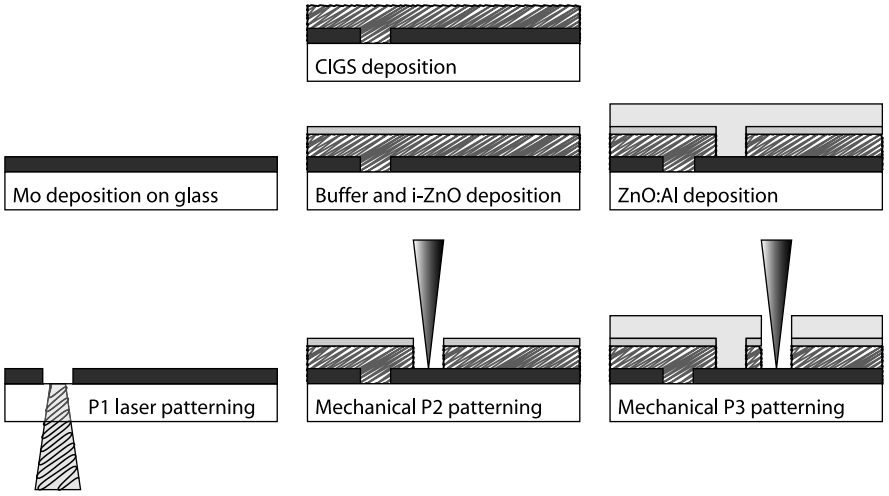

Figure 2.2: Sequential deposition and patterning steps used to form the monolithic interconnection

losses are significant and result in module efficiencies that are some 3-4 % units below that of cells, see for example [20].

2.3 Monolithic integration

In order to form the cell strips that make up a thin film PV module patterning steps are included between layer depositions. In Figure 2.2 the process flow is illustrated. The first patterning step (P1) is performed after bottom contact deposition, defining each individual cell width, see also Figure 2.1. Absorber and buffer layers are deposited, after which patterning (P2) opens up the via channel that connects adjacent cells in series when the top contact is deposited. Final (P3) patterning is performed to isolate adjacent top contacts. Creating this series connection within the structure itself is termed *monolithic* integration.

There are several methods available for patterning thin films. Using a light sensitive polymer mask, photolithography can be used to define etching regions in thin films and IC technology. It is a very high precision technology and could be used for large area applications such as PV modules [21]. However, the use of large amounts of chemicals and the batch nature of the process will have negative impact on its economics in the long term [22, 23]. Another issue with CIGS thin film technology is that the high temperature of the absorber deposition introduces some warping of the glass substrate. Due to these dimensional variations mask lithography becomes more difficult to control with precision.

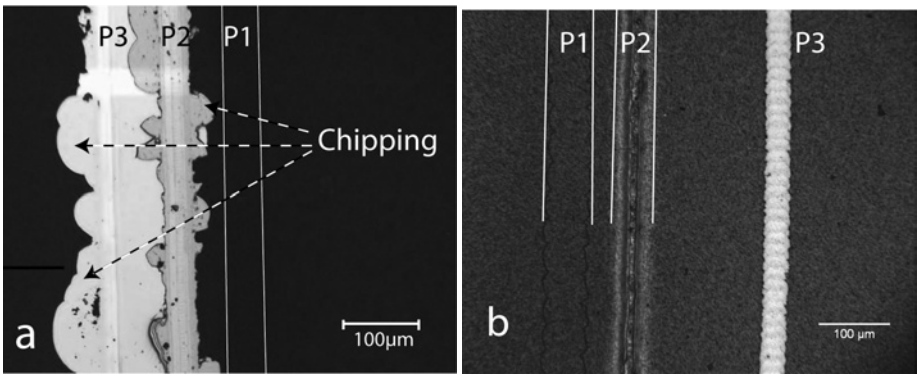

Figure 2.3: Micrograph showing the problem of chipping when using mechanical styli. (a) shows state of the art patterning and in (b) the advantage of all-laser scribing. Laser lines are straight and even. In this lab-scale example the P2-P3 scribe separation is excessive and not representative for an optimised process.

Mechanical stylus patterning is used for P2 and P3 in state-of-the-art manufacturing of CIGS thin film modules. It is a robust and simple process where the mechanical hardness of the bottom contact layer limits the removal to the softer semiconductor layers. While the initial investment is low, it does have drawbacks such as tool wear and machine downtime for needle replacement or redressing. Furthermore, a mechanically patterned line is not very well defined since adhesion of the individual layers affects the process and "chipping" is a common problem (see Figure 2.3a) resulting in widening of the patterning lines and need for increased line separation[24]. The final tally is a wider interconnect zone which translates to current losses in module power output (see previous section)[25].

Laser patterning is currently used for bottom contact P1 patterning in state-of-the-art CIGS manufacturing. There are some general advantages of laser patterning if considered as a replacement for mechanical patterning. Primarily, the laser lines can be made in a controlled and precise way due to the non-contact nature of the process, asserting no pressure on the substrate. This leads to straight and even pattern lines, see Figure 2.3b. The lack of physical contact also means that there is no wear of the tool and no replacement of needles with associated machine downtime is required. Laser patterning speed has been demonstrated as high as 4 m/s by using elongated laser spots and scanning mirrors [26]. However, full size panel patterning requires large motion systems to provide relative motion of beam and sample. Speeds as high as 2 m/s with high precision ($\pm$ 5 μm) have been reported[27].

2.4 The finished product

The final steps to ready a thin film PV module for installation and power generation involve adding terminal contacts, a junction box, encapsulation (usually in a glass-glass sandwich) and in some cases the addition of an aluminium frame. In order for encapsulation to be effective, semiconductor and metal films are removed around the perimeter of the modules, preventing humidity penetration and corrosion. This can be done by laser removal or by sandblasting the edges.

In Chapter 5 we will discuss some specific aspects of encapsulation and long term stability that are relevant to CIGS thin film PV modules.

3. Laser-material interaction

3.1 Laser basics

***L**ight **A**mplification by **S**timulated **E**mission of **R**adiation* - or *laser* for short - was predicted in 1916 by Einstein and experimentally achieved in 1960 by Maiman. A beam of laser light can be described as a way of delivering a well defined amount of energy across a distance in a very precise and localized way. In its cradle, the laser tool was very much a technology looking for an application. Since then it has found applications in abundance and variety. There are countless ways of utilizing this energy for diverse purposes ranging from communication and measurement to cutting and welding. Depending on the use there are many possibilities of tailoring the tool by selecting and/or tuning wavelength, pulse duration, repetition rate and output power. A short introduction is in order to aid in understanding laser as a tool for micromachining thin films as is the main purpose in this thesis. Where specific reference is not made, the descriptions within this chapter are based largely on two textbooks, references [28] and [29].

3.1.1 Basic laser components

Any laser will consist of at least three distinct components whose nature will determine all of the key properties of the laser beam and thereby its principal utility, see Figure 3.1. They are 1) an *active medium* in which the laser light is generated, 2) a *reflective* cavity within which light energy is amplified and 3) an *energy source*, supplying the active medium with energy that can be transformed into coherent radiation. Additionally there will be any number of external components in the beam path for focusing, shaping and guiding the beam to its target as well as internal components for wavelength manipulation etc.

The prerequisites for a lasing medium is that i) it can attain more than one distinct level of energy and that ii) the change from higher to lower energy states is a radiative process, i.e. that it loses its energy by emitting a photon of a specific wavelength. There can be several energy levels involved in the lasing mechanism, comprising both radiative and non-radiative processes and therefore some active media emit light at more than one wavelength.

One commonly used active medium is CO_2 gas, in the CO_2 gas phase laser. It attains its lasing from the vibrations of the CO_2 molecule which has three basic configurations depending on its energetic state. Molecular vibrations are

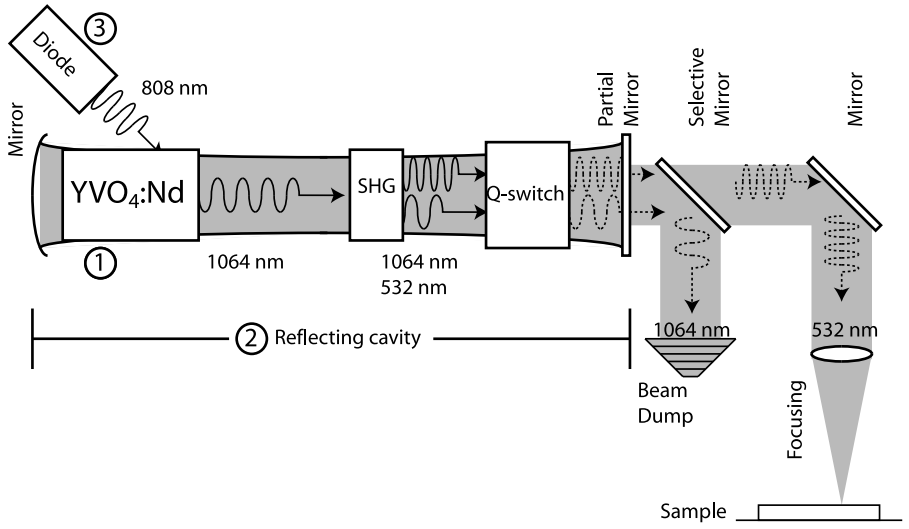

Figure 3.1: A schematic view of a laser set-up including the principal components active medium (1), reflecting cavity (2) and radiative pumping (3).

a relatively low level of energy and the CO_2 laser wavelength is far into the IR at 10.6 μm. On the other side of the spectrum the active medium is an *excimer*, a meta-stable molecule consisting of a halogen atom temporarily bonded to a noble gas atom. The excimer breaks apart radiating a high energy photon in the UV range. In a *solid state laser* the lasing medium is suspended in a solid, most commonly a crystal but glass is also used. In the section below we will take a closer look at the neodymium solid state laser type used for the most part in this work.

The cavity in which the active medium is placed serves to amplify the intensity of the laser light by internal reflection. Each reflection and additional passage through the active medium stimulates the emission of more coherent photons, amplifying the intensity of the generated radiation. Design of the cavity mirrors will affect the utilisation of the active medium as well as the spatial distribution of the laser light.

Energy is supplied to the active medium from an appropriate source. Gas phase lasers often utilise electrical discharge as source of energy that excites the medium to its higher but unstable state. For the solid state lasers pumping is done via radiation. Nowadays, pumping of solid state lasers is preferably done by semiconductor laser diodes since this enables better utilisation of the input energy and less thermal effects due to excess radiation introduced by flash lamps.

3.1.2 Neodymium type solid state laser

A very common type of laser used in processing of thin films, and throughout the experimental work presented here, is the neodymium laser. It uses Nd^{3+} ions trapped in a transparent solid as a lasing medium. The excitation of Nd^{3+} ions results in a radiative emission in the infrared, specifically 1064 nm or 1.16 eV. Its energy diagram is shown in Figure 3.2. Different crystal matrices are available, most commonly *yttrium aluminium garnet* (YAG) and *yttrium vanadate* (YVO_4). Pumping of the crystal rod is achieved by single wavelength light generated by (a) semiconductor laser diode(s) directed into the rod. The set-up used in this work has a pumping diode wavelength of 808 nm as illustrated in Figure 3.1. By using diodes instead of flash lamps the overall electrical efficiency is drastically increased while requiring less cooling of the crystal.

3.2 Additional components

3.2.1 Second harmonic generation

While the lasing medium determines a native wavelength of the light generated in the resonance cavity, a non-linear optical element can be

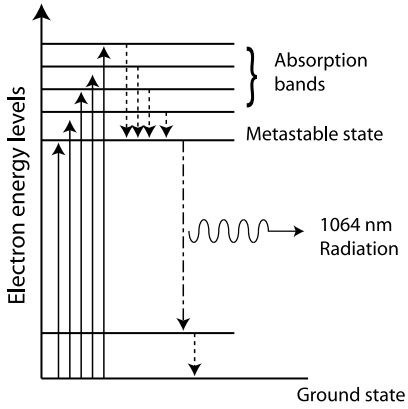

Figure 3.2: Electronic energy levels in neodymium adapted from [28]. Electrons are excited above the meta stable state (solid lines). Energy is released as heat as electrons drop down to the meta stable state (dotted lines). From the meta stable state energy is released by radiating a photon at 1064 nm wavelength (dash-dot line).

used to achieve so called second (third, forth..) harmonic generation, i.e. up-conversion of the photons to higher energies. For example, in a Nd:YVO_4 solid state laser, the native wavelength is 1064 nm infrared light. An external crystal of $LiNbO_3$, carefully placed and maintained at constant temperature, converts the light to the double frequency, 532 nm green light [28]. This conversion is done with considerable losses, in the order of 60-80 % and the output beam, which contains both wavelengths, must be filtered if only green light is desired for processing.

3.2.2 Pulsed laser and Q-switching

Efficient processing has proven to be aided by gathering the laser energy into very short pulses of high power. While pulsing of some systems can be achieved by pulsing the pumping energy, most solid state lasers used in processing rely on the use of a *Quality switch* or *Q-switch*. The Q-switch is placed in the beam path and operates by switching between an *open* and a *closed* state at a rate which can be controlled. As an example, the Q-switch in the system used in this work consists of an acoustically active crystal whose transparency depends on a RF bias across the crystal. Control of this bias will in turn control the pulse frequency - or repetition rate - of the laser output. The pulse duration is also given by the Q-switch and is generally not tunable but depends on the selected repetition rate. Q-switching can be achieved in a large range from 1 to hundreds of kHz with pulse durations down to 20 ns. To achieve higher pulse repetition rates and ultrashort pulse duration one must

consider such techniques as mode-locking. We will not treat mode-locking in this thesis and the interested reader is referred to [30].

3.2.3 Beam path and focusing

The output laser beam is (typically) of a near Gaussian spatial distribution that is far below the threshold density for damage of most inorganic materials (although it can still be very harmful for organic tissue). This is advantageous since it minimises the risk of damaging any optical elements used for guiding or focusing the beam or for measuring its characteristics. In the case of building larger and higher power laser systems this is a great advantage since it permits one to guide the beam by small and light-weight optical components while the laser cavity can remain on a stable platform. The beam is guided, via lenses or mirrors from the cavity to the surface of the sample. As a last stage in the beam path the focusing optical element is placed, which concentrates the beam to a very small diameter (typically 25 μm - 100 μm [31]) that has an energy density of necessary magnitude.

If no special lenses are employed, the laser spot will have an energy distribution in space, or laser *fluence* [J/cm^2], which is near Gaussian, see Figure 3.3a. For material processing there are fluence thresholds that define useful energy density for a desired process, whether it be ablation or transformation of the material. The Gaussian distribution is far from ideal for this purpose. The edges, or tails, of the energy distribution will be below the threshold for the desired interaction but will still deposit significant levels of energy to the film. At the center, there is a significant energy peak where the fluence will be above the threshold and where undesired effects such as damage to underlying film(s) or substrate may occur. One way to work around this is to use a *diffractive optical element* to redistribute the energy in the beam in a way that more resembles a uniform fluence, a so-called "top-hat" distribution, see Figure 3.3b [32]. If such a distribution is used, one can better utilise the laser energy [33] and both edge and center effects of an unwanted nature can be reduced [34].

3.3 Laser patterning

Laser-material interaction for micromachining takes place in three main steps: 1) Absorption of radiation in the material, 2) heating of the material and 3) removal or transformation of the material. In case of material removal the term laser *ablation* is commonly used. Material transformation can mean various different processes such as annealing, melting and recrystallisation or partial evaporation. We will now briefly consider the steps involved in micromachining of thin films. While the work presented here has been done with a device oriented approach, we will cite some particular relationships and magnitudes

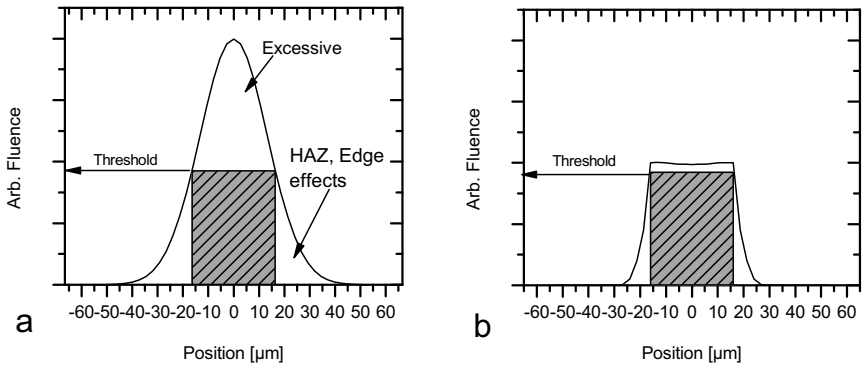

Figure 3.3: a) Gaussian energy distribution leads to excessive laser fluence at beam center and heat affected zones at the beam edges. b) Beam shaping increases energy utilisation while minimising unwanted edge effects and damage at beam center.

that will help reasoning on the experimental results presented in Chapter 4, particularly the use of subnanosecond ("ultrashort") laser pulses.

3.3.1 Absorption

According to the relationship between material properties and light absorption that was introduced in Section 1.3.1, laser light absorption will depend on the band gap of the material and on free electrons. Initially, a certain portion of radiation will be lost at the top surface (or interface in the case of stacked layers) due to reflection. The remaining part which passes into the material is termed its absorptivity. Absorptivity is wavelength dependent and defined as:

$$A(\lambda) = 1 - R(\lambda) - T(\lambda) \tag{3.1}$$

R(λ) is the reflectivity and T(λ) the transmissivity of the material. Typical spectral absorptivity curves for Mo, CIGS and ZnO:Al are given in in Figure 3.4. Obviously, it is important to consider the absorptivity of a material when selecting the processing wavelength. For the experimental work we have only employed the 2^{nd} harmonic wavelength (532 nm) of Nd^{3+} which corresponds well to absorbtivity of CIGS and Mo.

All the radiation energy is not absorbed immediately at the surface/interface. Absorption inside a material follows Beer-Lamberts law and the declining intensity into the material is given by [28]:

$$I(z) = I_0 e^{-\alpha \cdot z} \tag{3.2}$$

where α is the absorption coefficient of the material. The depth into which laser light reaches before being fully absorbed is called the *penetration depth*.

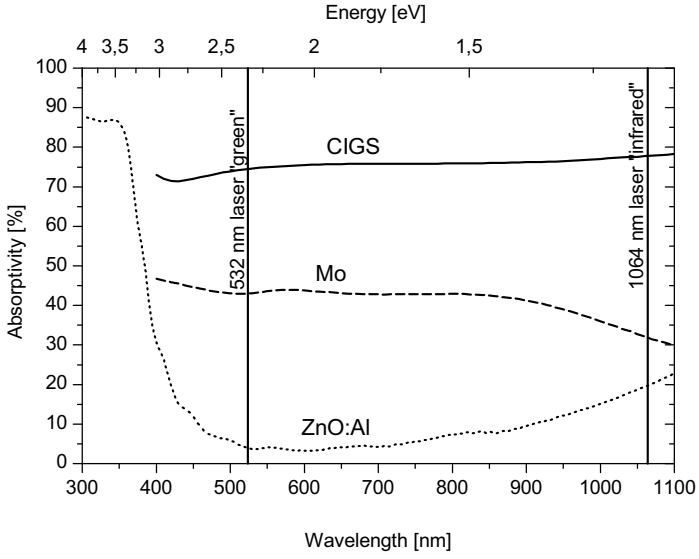

Figure 3.4: Absorptivity curves of ZnO:Al (dotted), CIGS (solid) and Mo (dashed) from UV to infrared wavelength. The native and second harmonic wavelengths of neodymium type solid state lasers are also included.

Typical values for opaque materials is in the range of 10 nm [35, 36] while calculations in PAPER I showed that for a transparent zinc oxide, the optical penetration depth for 1064 nm laser wavelength is $\approx 10\mu$m. In practical terms this means that selective energy deposition in the ZnO layer is very difficult at such wavelengths. If UV wavelengths are used, where ZnO is no longer transparent due to band gap absorption one can reach shallow penetration depths.

3.3.2 Heating

The energy absorbed by electrons within the penetration depth will rapidly be transferred to the atomic lattice and transformed into heat. Heat transfer by relaxation occurs in the order of picoseconds [35]. For nanosecond laser pulses, one can therefore consider the laser as a heat source in the penetration depth and heating of the surrounding film(s) and substrate will occur due to thermal conduction during the pulse. Heat diffusion distance is given by [37]

$$d_{th} = 2(\chi \tau_{las})^{1/2} \tag{3.3}$$

where χ and τ_{las} are the thermal diffusivity and the laser pulse duration, respectively. This illustrates the importance of pulse duration when attempting to minimize edge effects that issue from heat conduction. If laser pulses in the

same order of magnitude as, or shorter than, the relaxation time are used this relationship is invalid and the process becomes more complex to predict. The common way to treat modelling of such interaction is by a *two-temperature model* where electron and lattice temperatures are not in equilibrium, and diffusion of "hot" electrons comes into play. It is beyond the scope of this thesis to go into modelling and simulations of laser-material interaction but more can be found in references [38, 39].

3.3.3 Material removal - ablation

The removal of thin films is commonly referred to as *ablation*, from the Latin *ablationem*, "a taking away". Other, more ambiguous, terms used are *scribing*, *micromachining* or simply *patterning*. In this work we consider patterning as an all encompassing term referring to any process used for monolithic integration, ablation being one of them. More on this in Chapter 4.

Heating of the film continues until it reaches melting and eventually evaporation temperatures. With evaporation the material expands very rapidly and a recoil pressure is created as the vapor is ejected from the substrate creating a plume of gas or plasma, depending on the state of the heated matter. The recoil pressure will be directed down toward the substrate as well as toward the perimeter of the irradiated spot. Recoil pressure action can aid in removal of melt-phase material but can also damage the substrate or underlying films.

While some consider material removal to occur when the entire volume to be removed has reached the melt state [40], there seems to be some uncertainty as to the exact nature of material removal through laser ablation. Kim et al. pointed out that for ultrashort (picosecond) pulses neither the optical penetration depth nor the thermal diffusion length reaches far enough into the material to melt the entire layer thickness, and yet all material is removed [41]. It is suggested that ablation depends on many factors such as film-substrate adhesion, film cohesion, thermal expansion matching etc. A similar relation occurs for nanosecond pulses when laser energy is deposited at the substrate/film interface and ablation occurs before enough energy is deposited to melt the entire film. This can be explained by the fact that any expansion is enclosed and therefore can result in disintegration of solid film layers by thermal strain even if only a thin layer has been melted or evaporated[38].

3.4 Uses of lasers in photovoltaics

In the next Chapter we will focus on the use of lasers for patterning of thin film solar cells. Before we go on, let us just consider a few other examples which illustrate the versatility of laser processing and the potential uses of lasers in PV. Lasers have become an important part of the race to improve the efficiency and cost reduction of PV power generation. One established technique is edge

isolation scribing of the emitter region of wafer cells [42, 42, 43]. It has been suggested that laser soldering may result in better quality contacts for wafer cells [44] and it is also possible to use laser scribing or cutting to shape wafer cells [43]. Front grid metallization can also be done by laser treatment [45]. Definition of diffused base and emitter regions by laser ablation as well as opening of passivating layers have been presented [46]. Concepts that aim for increased efficiency cells, so-called novel concepts, include scribing wafer cells for deposition of buried contacts to minimise surface shading [47], back side *laser-fired contacts* that reduce the need for shading contacts on the cell front [42], similar to *emitter wrap through* which can be achieved by laser drilling [43]. Laser surface treatments can be used to reduce reflectivity of cell surface and increase light trapping in multi- and monocrystalline Si solar cells [48]. A relatively recent development is to crystallize thin films of a-Si to form *crystalline silicon on glass* (CSG) using layered laser crystallisation (LLC)[49].

3.5 Conclusion

We can conclude that laser ablation of thin films is a very complex process which is difficult to predict and model with certainty. Experimental work is absolutely essential when it comes to patterning of thin film solar cells, particularly to determine electrical isolation or short-circuits between the layers. It remains clear however that the shorter the pulse duration, the less thermal effects should be expected, particularly at the edges of the laser irradiated spot. Edge effects and unwanted damage at beam center could also be minimised by controlling the beam shape and laser energy distribution.

4. Laser patterning in thin film photovoltaics

Now that we know something about what lasers can do, we will see what lasers can do for thin film photovoltaics. Laser processing is now established as an enabling technology in the manufacturing of thin film PV modules, particularly for a-Si and CdTe technologies. The advantages that were introduced in the previous chapters such as narrow features [24], little stress, low downtime and running costs [23] all help to achieve high throughput and high yield in the production of thin film PV modules, ultimately resulting in a good cost structure. This chapter will go through some specific challenges and possibilities involved in using laser patterning to achieve the monolithic integration of CIGS solar cells into large area modules. The techniques used, along with relevant module results, are summarized in table 4.1 at the end of this chapter.

The most straight forward task is to ablate a single thin film deposited on a substrate. As more layers are deposited, the challenge becomes to achieve removal - or transformation - of the desired layer without detrimental damage to other layers or in any way compromising the functionality of the cells or the monolithic interconnection. As we will see below, this depends greatly upon the properties of the individual layers in the stack and therefore solutions for one PV technology will not necessarily be applicable to others.

4.1 Ablating single layers

By single layer ablation we refer to the removal of a thin layer from a substrate whose thickness vastly exceeds that of the layer to be removed. Single layer ablation can be performed from the film side - *direct ablation* - with the laser beam incident on the top surface of the film to be removed, Figure 4.1a. *Direct induced ablation* on the other hand occurs when the laser is incident through the substrate - provided that the substrate is transparent to the laser wavelength employed - depositing the laser energy at the substrate/film interface, Figure 4.1b. By depositing the laser energy directly at the substrate/film interface it is possible to achieve higher ablation efficiency, see e.g. [26, 38, 50]. This is due to the fact that evaporation of only a thin layer at the interface and the subsequent expansion removes the rest of the film. Since the beam passes through the substrate, it avoids absorption losses in the gas/plasma plume which is present for direct ablation. The laser optics are also protected from these ejec-

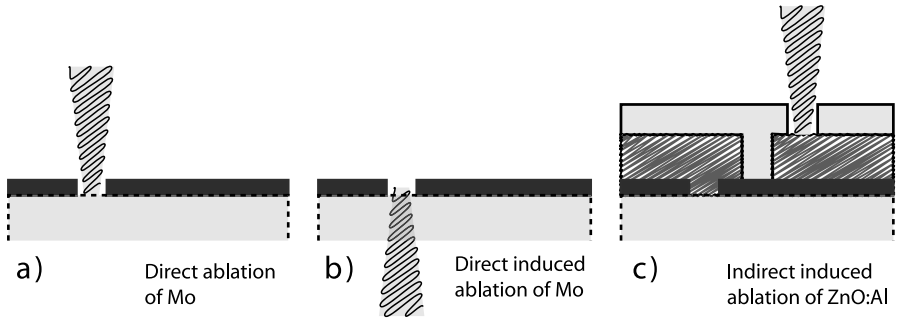

Figure 4.1: Three main ways of achieving ablation. Direct ablation deposits energy directly to the film that is to be removed. Direct induced ablation deposits energy at the film/substrate or film/film interface, blasting off the topmost film. Finally indirect induced ablation blasts off the topmost transparent film by laser absorption and evaporation of the layer below.

tion phenomena by the substrate [27, 50]. Success of the process will depend on the absorptivity of the film and the film/substrate adhesion. Of course, direct induced ablation requires that the substrate back surface is completely free from scratches, dust or any other disturbance that may affect the beam. It has been put forth that handling is more difficult when the laser beam is to be directed from the back of the substrate.

If the film to be removed is transparent but the substrate is highly absorbing one can sometimes achieve *indirect induced ablation* with the beam incident through the transparent top film. Ablation of a thin fraction of the absorbing material removes the layer on top by the force of evaporation similar to direct induced ablation. This is of course also possible for stacked layers if the underlying film is highly absorbing, as illustrated in Figure 4.1c.

4.1.1 Mo bottom contact

In the case of CIGS solar modules, the first contact layer is a molybdenum metal with a thickness in the range of 0.3 - 1 μm deposited by magnetron sputtering onto a substrate. There are several choices for substrate, and soda lime glass is by far the most common while metal [19, 51] and polymer [51, 52, 53, 54] foils are used to produce flexible and light-weight PV devices for portability and/or integration in products or buildings. It is noted that most manufacturers working with such substrates work with wafer-like module technologies where monolithic integration is not used. Absorptivity in Mo is moderate for both the native (1064 nm) and second harmonic (532 nm) wavelengths of Nd:YAG and Nd:YVO_4 lasers, see Figure 3.4. Due to the losses involved in second harmonic generation scribing is predominantly done using the native wavelength. Since soda lime glass, which is the most common substrate for CIGS modules, is transparent at the relevant wavelengths,

there is the aforementioned choice between direct ablation or direct induced ablation. Advantages of direct induced ablation that have been reported for molybdenum thin films used for back contacts in CIGS technology include improved scribe edge appearance [26] which was also one of the conclusions of my MSc thesis [55]. To the best of the authors knowledge direct ablation is still preferred by manufacturers, presumably due to complexities involved in laser incidence from the substrate back side and the risk of dust and scratches disrupting the scribe line integrity.

4.2 Ablating stacked layers

As we know from the introduction, thin film solar cells are structures of thin layers stacked on top of each other to form a complete cell. The interconnection of these cells requires that intermediate patterning can be performed in a selective manner, i.e. where at least one layer remains undamaged by the patterning process. With the state-of-the-art metal stylus patterning of CIGS thin film solar modules, the selectivity stems from mechanical hardness of the Mo contact which is superior to that of the semiconductor layers deposited on top, i.e. CIGS/CdS/ZnO/ZnO:Al. The metal stylus scribes a line along the surface of the device with a pressure that is controlled to ensure that a) all of the semiconductor material is removed and b) no damage is caused to the Mo contact. This requires a high degree of pressure control and regular replacement of metal styli [25]. Furthermore, the method limits the speed of the process due to the low tolerance to discontinuities in the scribe line which can introduce short circuits between adjacent cells.

While CIGS manufacturing for the most part usses the metal stylus method[1], the sibling technologies of a-Si and CdTe have implemented laser patterning for all the patterning steps[2]. In order to understand why we must consider the technical difficulties that separate the technologies. The main technological divider is the use of a superstrate structure for CdTe and a-Si and the consequent transparency of the first deposited layer[3]. The first patterning step of this transparent bottom layer differs only little from the case of Mo. It is mainly a matter of compensating for the low level of absorptivity in the transparent contact by increasing the fluence of the

[1] With the exceptions of monolithic integration on flexible substrates where the metal stylus method is impossible due to ease of damage to the substrate. More on this in the coming Sections.

[2] In some cases metal scribing is cited for CdTe[56].

[3] Some confusion can arise at this point. "Substrate" is taken to mean that the support material (glass) is at the back of the solar cell, facing away from the sun. "Superstrate" is taken to mean that the support material at the front of the solar cell, facing the sun. To be clear, this text and illustrations refer to the respective layers as *bottom* always meaning closest to the support material and *top* furthest from the support material. Hence, a superstrate cell must have a transparent bottom contact to allow light through to the absorber.

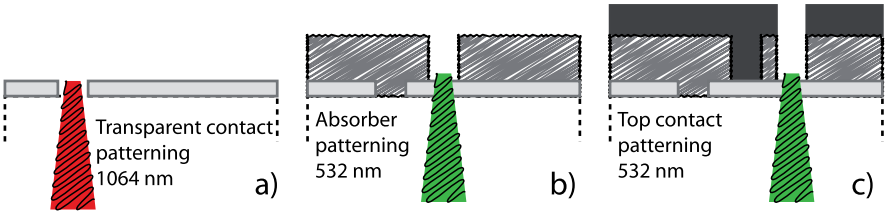

Figure 4.2: For the sibling technologies, CdTe and a-Si thin film PV, all laser processing is common. A key contributor to this is the transparency of the first layer which allows direct induced ablation of the absorber (P2) and absorber/contact (P3) layers. By changing wavelengths, this selectivity is enhanced.

incoming laser beam. And since there are no absorbing materials in the stack the high power level is not a problem. After the absorber layer is deposited the bottom contact transparency becomes a great advantage from a processing point of view. It allows manufacturers to use a similar strategy as for the single layer approach. With the laser beam incident through the substrate *and* the transparent contact direct induced ablation can be achieved, see Figure 4.2b. Since the absorber layer has a high absorptivity, and since direct induced ablation requires less energy than direct ablation, it will reach ablation conditions at a level of fluence well below that used for patterning the transparent contact. This selectivity by ablation threshold can be enhanced further by the choice of processing wavelength. E.g. the first patterning step in a-Si module integration is done with a native (1064 nm) wavelength Nd:YAG laser and subsequent patterning uses the frequency doubled (532 nm) wavelength where TCO absorption is even lower [27, 57, 58, 59]. The same strategy is valid for CdTe [60]. As an example, values given in [61] place these fluences at 4.5 J/cm^2 for FTO and 0.1 J/cm^2 for CdTe.

Furthermore, since the final deposited layer is on top of the absorber, the exact same processing conditions are valid for the third patterning step [57]. As the absorber reaches ablation at the TCO/absorber interface, the explosive removal of the aborber will automatically remove also the top contact layer, see Figure 4.2c.

4.2.1 CIGS P2 scribing by direct ablation

For CIGS thin film solar modules, the P2 and P3 scribes cannot be performed by direct induced ablation due to the substrate configuration and choice of a non-transparent bottom contact. Therefore any removal of CIGS to open up the P2 connection via must be done top-down. Several commercial and research efforts have been presented on the topic, showing considerable difficulty in limiting the laser ablation at the Mo/CIGS interface. Compaan et al., who published a comprehensive study using a range of lasers and materials,

concluded that ablation of CIGS is challenging due to the small difference in damage threshold for CIGS and Mo. None of the evaluated laser configurations allowed for selective removal of CIGS without damage to the underlying Mo layer [61]. Mo damage and edge melt effects when using ns laser for direct CIGS ablation has since been encountered by others [41] and the trend is toward using ultrafast laser pulses to achieve selective removal of CIGS. Pico- and femtosecond laser pulses have a shallower interaction depth [41] and can therefore be used to ablate thin layers in a more controlled manner than is the case for nanosecond laser pulses. Using ultrafast lasers to remove CIGS without damage to the molybdenum and with minimal edge effects has been reported [62]. Edge effects are avoided due to the ultrafast interaction with the material minimizing the thermal conduction during material ablation and therefore minimizing the heat affected zone along the edge of the laser scribe.

4.2.2 CIGS P3 scribing by direct ablation

With the complete stack of layers deposited, the P3 scribe is necessary to isolate adjacent front contacts. Referring again to the state-of-the-art mechanical removal, this is achieved by scribing a line that is self-limiting at the Mo surface, analogous to the P2 scribe. When performing this final mechanical patterning step, removing the CIGS is a consequence of the method used rather than a necessity. In fact, as we have shown in PAPER II, the exposed and scratched molybdenum surface in the P3 scribe is highly susceptible to corrosion and was the section where test structures reached complete circuit disruption during exposure to a damp heat stability test (see Section 5.1.2). It would therefore be considered an advantage if P3 could be performed by isolating the zinc oxide contact without exposing the molybdenum.

The topmost ZnO:Al contact layer has low absorption for visible and IR wavelengths where the typical Nd laser systems operate. However, as was pointed out by Compaan et al. [61], absorption is high at UV wavelengths (Figure 3.4). They showed successful and controlled results using direct ablation of ZnO:Al on glass using excimer lasers. There is the possibility to utilise 4^{th} harmonic generation of the Nd:YAG native wavelength 1064 nm resulting in a 266 nm UV beam which is more readily absorbed by the ZnO:Al layer. It has been shown that such a setup can successfully ablate ZnO:Al layers deposited on glass. However, ablation of ZnO:Al on top of the cell stack resulted in direct ablation of both CIGS/ZnO:Al due to the higher absorptivity in CIGS [63]. This experience seems to be universal, and the use of direct ablation to *selectively remove* the top ZnO:Al contact is unlikely to be achieved with an industrially attractive system. Meanwhile, there are reports showing that direct ablation of *all semiconductor layers* is a more likely process, although problematic. Since it is similar to P2 by direct ablation, similar problems are encountered such as damage to the Mo layer and edge effects. Residual melt

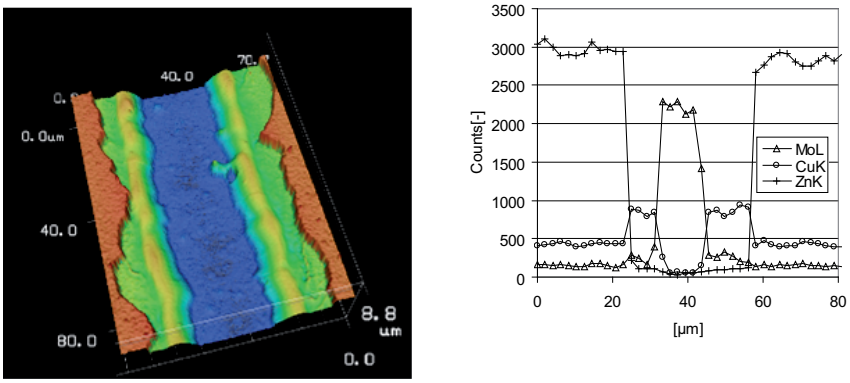

Figure 4.3: Left: Confocal Laser Scanning microscope image showing the appearance of a P3 scribe line by direct ablation of CIGS/CdS/iZnO/ZnO:Al. The ZnO edges are well defined and abrupt, ensuring isolation across the scribe even though some melt phase appears at the CIGS edge. Right: EDS scan across the P3 scribe line.

phases that compromise the isolation of the scribe have been reported when using nanosecond lasers [64].

In the work presented in PAPER I we approached the challenge by using a picosecond laser to minimize the thermal effects. With less heat conduction during the pulse, both laterally and depth-wise, we were able to achieve reasonable selectivity of the scribe. Even so, we identified considerable edge effects and process control was difficult with cracking of the Mo film evidenced for some samples. We concluded that scribe isolation was achieved due to the sharp edge of the ZnO:Al layer that did not overlap with the affected CIGS edges, as evidenced by EDS (Figure 4.3). Similar experiences have been reported [53] and others indicated that even with apparent edge melt the electrical results can be good [65]. The thin film modules manufactured using this type of P3 isolation scribes were fully functional. However, they appeared to suffer from reduced fill factors which we attribute to shunting at the thermally affected scribe edge. Additional isolation using mechanical scribing improved the device fill factors, especially those which performed poorest. However, there was also some improvement for a module which did not receive additional isolation. This may be related to temporary performance degradation incurred during storage and handling and suggests that part of the improvement for mechanically isolated modules was not due to problems with the laser patterned P3. The best device performance, which was not explicitly stated in PAPER I, is shown in table 4.1.

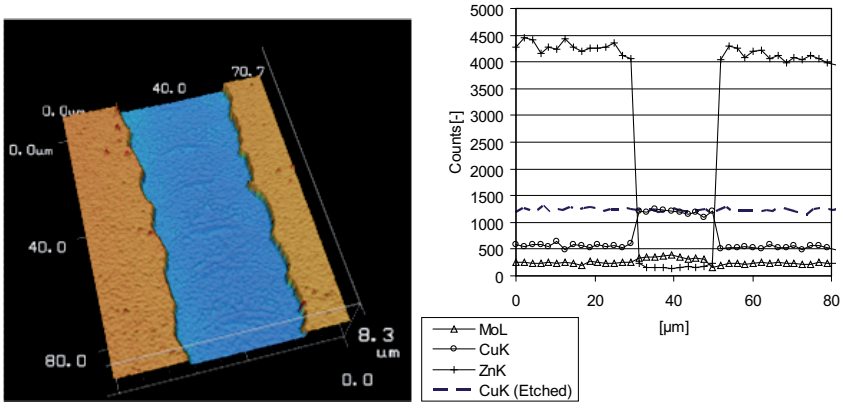

Figure 4.4: Selective P3 scribing by indirect induced ablation. Left: Confocal scanning microscope image showing the 3D profile of the P3 scribe. Right: EDS scan across the scribe line. The dashed line shows the results of EDS after etching away the ZnO:Al and highlights that no change in composition was detected in the laser treated area.

4.2.3 CIGS P3 scribing by indirect induced ablation

The difficulty in achieving successful direct ablation of ZnO:Al or CIGS/CdS/iZnO/ZnO:Al may not be such a huge tragedy. In fact, there is an alternative that looks both easier and less demanding on the equipment side while resulting in the preferential selective removal of ZnO:Al. Since the use of picosecond lasers minimizes the penetration depth it is possible to evaporate a thin fraction of the CIGS at the CIGS/ZnO:Al interface, see illustration in Figure 4.1c. This type of process can generate enough vapor phase to induce ablation of the top layer, effectively blasting it off, while only causing some moderate surface modification to the CIGS layer, see Figure 4.4. In PAPER I we presented work on CIGS modules P3 patterned by indirect induced ablation. Our main conclusion was that we could achieve good isolation and found no evidence of compositional changes in the CIGS surface where laser ablation had occurred. This process used a low pulse-to-pulse overlap (<50 %) which is consistent with high speed processing. Others have reported the same experience [26, 66].

4.3 Alternatives to ablation

Keeping an open mind, the change from a mechanical stylus tool to a laser beam is not a mere replacement with benefits such as narrower machining and less maintenance requirements. Laser tooling is also vastly more versatile in terms of the type of material interaction that can be achieved. In this section

we will consider some available choices for patterning in CIGS thin film solar module integration that are unique to laser processing.

4.3.1 CIGS P2 scribing by material transformation

From previous sections we have become acquainted with the challenges and opportunities that are involved in using a laser tool for removing material altogether. However, the highly thermal nature of nanosecond laser patterning is also capable of locally transforming the CIGS semiconductor compound into a conductive compound, see illustration in Figure 4.5a. It has been shown by some groups attempting direct ablation of CIGS that a residual transformed "CIGS" phase can be allowed as it is "more or less conductive" [52], while other have reported a specific contact resistivity[4] around 1 ohm·cm [67]. Others have found that laser processing gives lower contact resistivity compared to mechanical scribing; 0.1 ohm·cm and 0.6 ohm·cm respectively [68]. It must be stated that in this case there was no explicit demonstration of the nature of the laser patterned CIGS.

In PAPER III we have shown that transformed CIGS can be used for interconnections. Thin film PV modules were manufactured with a laser patterning process using a 532 nm ns laser. Instead of direct ablation, interconnection is achieved by local laser treatment to form a conducting line which connects back and front contacts electrically. Devices using this form of interconnection showed electrical performance equal to the mechanically patterned references and the best device reached a module aperture area efficiency of 15 %, see Figure 4.6. We also found contact resistivities of the transformed interconnect to be 0.4 ohm·cm, which was higher than what we found for mechanically patterned interconnects, 0.1 ohm·cm. While this may seem like a relatively large increase, the effect on output power will be mild. At standard irradiation it correlates to voltage drops of 6 mV and 1.5 mV repectively in a cell which operates between 500-550 mV. An increased voltage drop of about 1 % would be incurred by this increased resistivity. We note here also that work presented in Chapter 5 found specific resistivity of mechanically patterned contacts at 0.7 ohm·cm.

Investigating CIGS samples with laser rastered surfaces we were able to use film characterization tools such as x-ray diffraction (XRD) and x-ray fluorescence spectroscopy (XRF) to investigate the effect of laser scribing on the CIGS material, see PAPER IV. The results showed that the laser treatment induced partial evaporation of primarily In and Se leaving the remaining material rich in Ga and Cu, Figure 4.6. At higher laser fluences the residual phase becomes very copper rich. The structure of the remaining material appeared to be mostly CIGS or Cu_xSe who share crystallographical arrangement and are therefore very difficult to distinguish. Some evidence from XRD suggested

[4] Specific contact resistivity disregards the surface area occupied by the contact and is given in *resistance·unit length*.

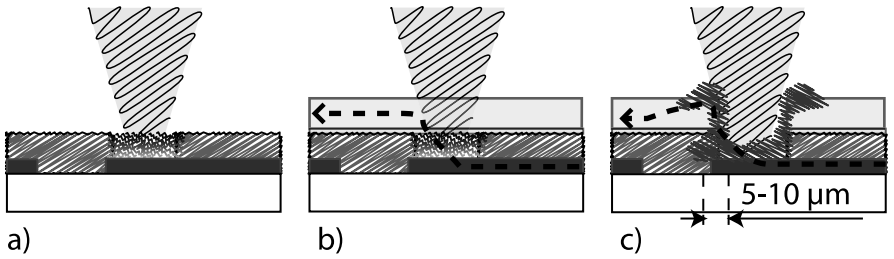

Figure 4.5: a): Laser P2 by transformation of CIGS into a conductive compound as described in Section 4.3.1. b): Conceptual drawing of the laser micro-welding process described in Section 4.3.2 as it looked before any experimental results were achieved and c): Illustration of current understanding of the resulting micro-weld interconnect.

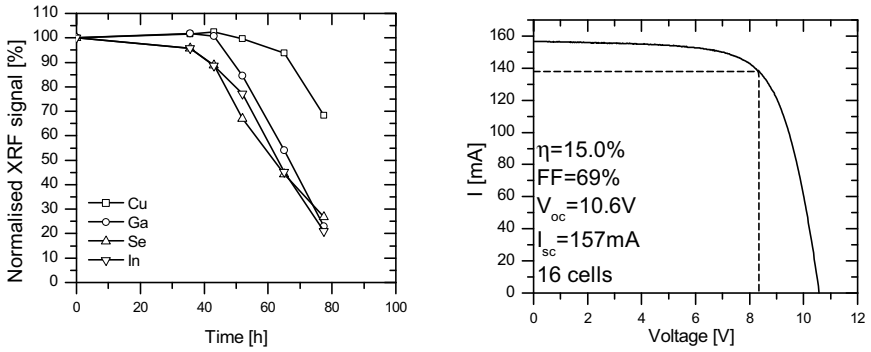

Figure 4.6: Left: XRF composition for a range of laser fluences showing that there is a selectivity with increased Cu ratio in the residual films. Right: Champion module manufactured with laser transformation patterning as interconnection technique.

the presence of Ga oxides after laser transformation. Segregation of Cu_xSe is one of the expected reasons for increased conductivity in the transformed material.

4.3.2 CIGS P2 scribing by laser micro-welding

Finally we will consider the use of laser for melting and welding of the CIGS stack layers. This is a method which breaks free of many limitations associated with the metal stylus patterning and offers considerable advantages on a manufacturing level. The work is presented in PAPER V and PAPER VI. The idea or concept of using the laser to form a welded contact was a development of our results on CIGS transformation to create interconnecting lines. The naïve thought process was that *"If we can make CIGS conductive using*

the laser, and the laser passes through the transparent contact, we should be able to form the P2 connection after ZnO:Al is deposited". While the concept drawing (Figure 4.5b) shows a solid transformed section of CIGS underneath an undisturbed ZnO:Al layer, we have found that the reality proved to be quite different (Figure 4.5c).

The proof of concept of the process was presented in PAPER V. Module samples were selected from several experimental campaigns with varying sources of CIGS material and in spite of the modest process knowledge, each experimental set contained several working modules. A comparative summary of module efficiencies along with IV curve comparison for a scale-up to 30x30 cm^2 sub-module is shown in Figure 4.7. The best results were comparable in efficiency to mechanically patterned references even though many suffered from elevated series resistances and FF losses. Since then, during the work with PAPER VI but not published therein, a champion mini-module with 14.0% efficiency has been manufactured, see Figure 4.8 and Table 4.1.

It appears that the function of the laser micro-welded interconnection is due to the same, or a similar, change in material composition as was shown for CIGS transformation above. However, the width of the effective region is in the order of 10 μm, considerably less than a standard mechanical scribe line which can be 40 μm at its narrowest. Using TEM with EDS, detailed analysis of the interconnecting region was performed. These results from PAPER VI showed phase separation of Cu_xSe as well as higher metallic content in the interconnecting region.

While the process appears controllable within a process window of laser fluences, there are some issues that remain to be clarified. In PAPER VI we could show how the process window defined by good electrical performance and working devices overlapped with extensive damage to both the Mo bottom contact and the glass substrate. Mo damage appears to be related to pulse energy and the maximum fluence at the laser spot center. Defocusing the beam to achieve flatter energy distribution in the beam resulted in higher thresholds for Mo damage. With this in mind, it may be possible to avoid the damage by using beam shaping optics that flatten the profile of the beam to a near top-hat distribution[32].

Glass damage on the other hand appears as a consequence of the thermal load on the substrate. Regardless of the distribution in the laser beam, all absorbed energy must either be emitted or dissipated in the substrate via conduction. Therefore, the threshold for glass damage does not depend on the pulse repetition rate or beam shape. However, as was found in PAPER VI, with increased ablation of the bottom contact a larger part of the laser beam will be transmitted without absorption which will decrease the amount of energy dissipated and therefore the damage suffered by the substrate.

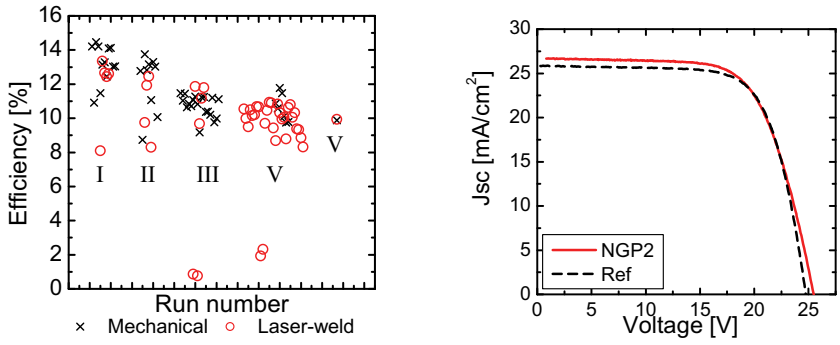

Figure 4.7: Efficiency of experimentally patterned modules compared to mechanically patterned references.

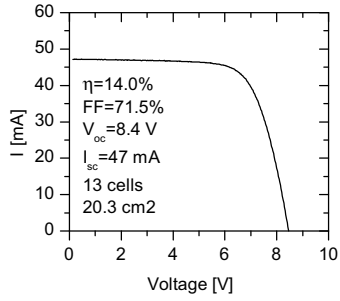

Figure 4.8: I-V curve and relevant characteristics for the champion CIGS module with microweld interconnection.

4.3.3 Advantages of micro-welding

With process control and electrical performance being such a challenge, it is important to underline the foreseeable advantages of introducing laser micro-welding as an industrial process when manufacturing CIGS PV modules. Consider the diagram in Figure 4.9. Standard process flow involves 3 pumping steps and 3 alignment steps. Introducing laser patterning to replace the mechanical patterning processes does not change this fact, even though it may increase the speed of the individual process. Once we achieve good reproducibility and control of the micro-welding process, along with the functioning laser process for P3 patterning, one can envision a combined patterning tool which would reduce P2 and P3 patterning to a single step with one single alignments step. Furthermore, if we for the sake of argument assume successful implementation of a vacuum based process for the buffer layer deposition (see for example [20, 69]), all semiconductor layers could be deposited in a continuous vacuum. This will reduce pumping times and most likely improve interface control in the deposition sequence. Improved solar cell performance by better control and less unnecessary exposure has been reported [70].

An international patent application has been made for the micro-welding method for interconnecting CIGS thin film PV modules.

4.4 All-laser patterning

We have shown the possibility of using laser methods for all patterning steps in CIGS PV module manufacturing. The reader can turn back to Figure 2.3 in Section 2.3 for a visual reminder of the gain when working with laser patterning. Shown in that image, laser micro-weld P2 width was 45 μm while the indirect induced P3 scribe line was 36 μm. Due to the fact that P3 was performed using an experimental patterning system, without the possibility of μm alignment, the P2-P3 separation is excessive. With the reported control of large patterning systems in the range <10 μm [27] this would add up to a total interconnect width of 45+10+45+10+36 = 146 μm or 2.9 % of the aperture area. While some report interconnect widths for mechanical patterning in the range 400-450 μm [25] we believe 250 μm could be reached, a range of 5-9 % of the cell area . This means an active area in the range 91 % to 95 % which laser patterning could increase to 97 %. Increased active area translates to higher current collection and power output. For example, this would bring the record module mentioned in Chapter 1 [14] from 97 W up to 101 W or from 14.2 % to 14.8 % aperture area efficiency, assuming an initial mechanical patterning width in the middle of the range, 350 μm.

We also note that both P2 and P3 patterning in Figure 2.3 were performed after deposition of ZnO:Al layer. While this has the promise of improving the cell stack (see above) and reducing processing times, these gains are less straight forward to quantify and are therefore left for future work.

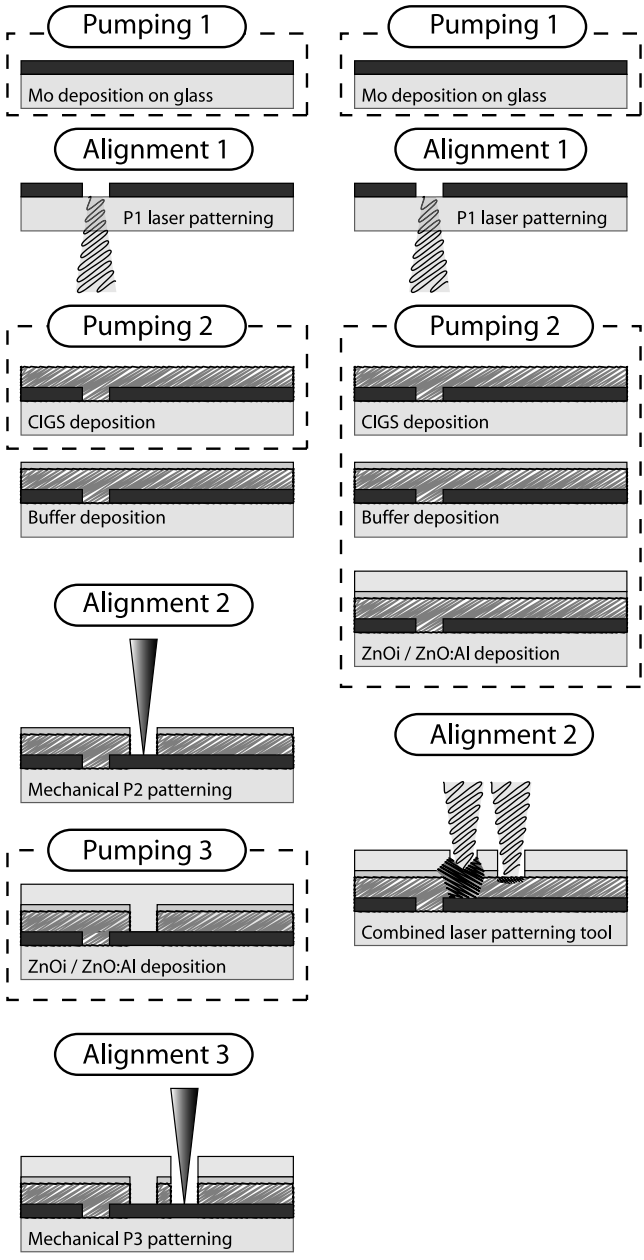

Figure 4.9: Left: State of the art process flow. Right: Foreseeable process flow with vacuum-based buffer layer deposition and dual laser patterning tool including laser micro-welding. Processing advantages such as better interface control for the semiconductor layers and reduced times for pumping and pattern alignment are predicted.

Table 4.1: *Overview of laser patterning techniques and publications*

Technique used	Layer(s)	Laser specs	Best Module		Reference		Published
			FF[%]	Eff[%]	FF[%]	Eff[%]	
Ablation							
P1 - Direct	Mo	ns @ 1064/532 nm					MSc. Thesis [55]
P1 - Direct induced	Mo	ns @ 1064/532 nm					MSc. Thesis [55]
P3 - Direct	ZnO/CIGS	ps @ 532 nm	60.1	10.0[a]	65.5 ± 2.8	10.6 ± 0.5	PAPER I
P3 - Indirect induced	ZnO	ps @ 532 nm	66.9	11.0[b]	65.5 ± 2.8	10.6 ± 0.5	PAPER I
P2 - Transformation	CIGS	ns @ 532 nm	69.5	15.0[c]	no ref		PAPER III
			63.7±2.8	12.8±0.7[d]	64.3±1.8	13.0±0.2	PAPER III
			75	14.5[e]	no ref		PAPER VII
			69.0	11.3[f]	68.9 ± 2.9	10.7 ± 0.7	unpubl.
P2 - Micro-welding	ZnO/CIGS	ns @ 532 nm	70.0	13.7[g]	72 ± 1.7	14.0 ± 0.3[h]	PAPER VI
			67.0	9.9[i]	71.0	9.9	PAPER V
			70.2	11.9[j]	68.9 ± 2.9	10.7 ± 0.7	PAPER V
			71.5	14.0[k]	72 ± 1.7	14.0 ± 0.3[h]	unpubl.

Reference performance reported as average values and standard deviations.
a - 16 cells, 14.4 cm^2 aperture area
b - 16 cells, 19.2 cm^2 aperture area
c - 16 cells, 80 cm^2 aperture area
d - Avg.(±StDev.) of 4 modules, aperture area 76 cm^2 cell count varied
e - 16 cells, 11 cm^2 aperture area
f - 16 cells, 77 cm^2 aperture area
g - 3 cells, 3.75 cm^2 aperture area
h - references are gridded lab cells
i - Scale-up: 46 cells, 589 cm^2 aperture area
j - 16 cells, 32 cm^2 aperture area
k - 13 cells, 20 cm^2 aperture area

5. Encapsulation and long term stability

While laser processing involves advantages regarding reduction of processing times and increase in power output of finished modules by decreasing the area loss inherent in monolithic integration we must also consider the lifetime of each module in order to gauge its commercial and energetic value. If you recall the chart in Figure 1.6, the lifetime is one of the key important properties determining the value - economic and energetic - of a photovoltaic module. The longer the lifetime, the higher the net gain in energy and also, the better the economy for the owner of the module.

5.1 Damp heat testing

In order to be competitive on the PV market it is imperative that manufacturers offer long term power output warranties (typically 80% output after 25 years, see e.g. [71, 72]). An example of long term performance for thin film CIGS modules in a 20 year field test can be found in [73]. Degradation was most apparent as increased series resistance attributed to degradation of the window layer and interconnections. From a commercial stand-point, long term field testing is not a viable option for qualitative evaluation of module lifetime performance. The solution to this is to perform *accelerated lifetime testing* that targets the expected weaknesses of the finished modules such as corrosion of contacts, load damage, delamination of encapsulation materials etc. This is especially relevant for any novel concept that is introduced to the market, as customer confidence in their return of investment is key for PV module installations. For this purpose one has developed a series of tests summarized in qualification standards. Initially, thin film and wafer-based modules were tested according to the same criteria but there is now a separately defined qualification standard for thin film modules published in the IEC standard 61646 [74]. An extensive review on the development and motivation for the included tests can be found in [75].

One of the most critical tests in the IEC 61646 qualification standard is the *damp heat* test where modules are submitted to a hot and humid environment (85 % relative humidity (RH) @ 85 °C) for the duration of 1000 h. In order to pass the test, modules must not only maintain their initial rated power output within 5 % but must also uphold cosmetic and mechanical integrity. For ex-

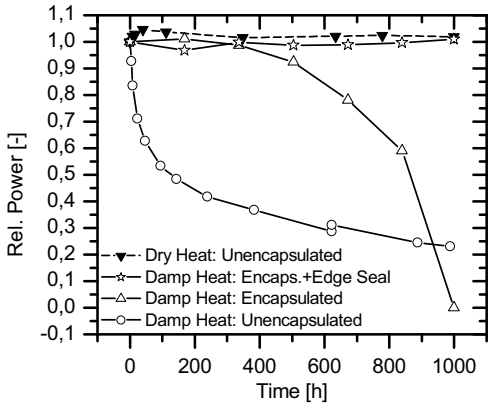

Figure 5.1: Module output degradation during stability testing. Damp heat testing degrades module performance rapidly (open circles). Single laminate encapsulation withstands degradation for a certain time but is not sufficient to protect the semiconductor layers from moisture ingress (open triangles). Edge sealed modules maintain stable output throughout the test (starred) as do unencapsulated modules if tested in dry heat (filled triangles).

ample bubbles appearing in the encapsulation material will rate the module as "fail" even if power output is maintained. Previous work in the research group showed that degradation of CIGS cells in damp heat will reduce primarily the V_{oc} and FF [76, 77, 78, 79]. Modules will suffer additional FF losses due to increased series resistance in the ZnO:Al contact and interconnect [80].

5.1.1 Encapsulation

While dry heat is not a problem for CIGS cells and modules, the high level of humidity in the damp heat test causes severe degradation of performance (see Figure 5.1. Therefore in order to ensure long term stability CIGS PV modules must be packaged or encapsulated in such a way as to prevent penetration of humidity. While wafer modules withstand somewhat more humidity and can be sufficiently protected if encapsulated by an *ethylene vinyl acetate* (EVA) adhesive film and a polymer back sheet, thin film modules require additional protection. The glass-glass laminate is therefore commonplace for all thin film technologies. We found that, even with the perfect (in practical terms) barrier properties of the glass sheets, harmful amounts of humidity can still enter the encapsulation at the edges. In PAPER II we showed that adding an additional barrier around the edge of the module is necessary to block entry of harmful levels of humidity. Modules with edge sealant passed the 1000 h damp heat test with maintained output power. These results are shown in Figure 5.1

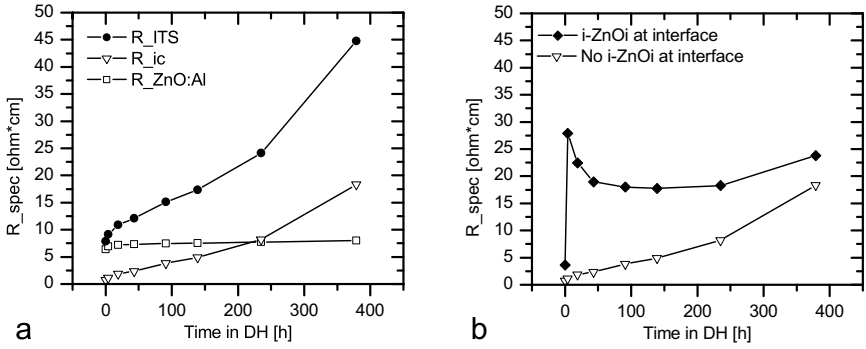

Figure 5.2: a) Interconnect test structure total specific resistance increase in damp heat. Subtracting the increased resistivity of the contact layers from the total resistance resulted in an estimated contact resistance in the P2 scribe line. At 400 h exposure the structure resistance rose to extremely high levels due to complete corrosion in P3. b) Specific contact resistance extracted from interconnect test structures in damp heat with i-ZnO in P2 (filled symbols) and without i-ZnO in P2.

5.1.2 Importance of interconnects

We also attempted to determine the importance of series resistance degradation in the interconnects during damp heat exposure. Special interconnect test structures (ITS) were included in the damp heat test, and the results showed how contact resistance rises strongly during the first 400 h of the test, see Figure 5.2a. At 400 h the structures failed completely and inspection revealed complete corrosion of the Mo layer in P3. Parallel testing of single layers corroborated this as Mo films maintained a low sheet resistivity, even when visibly degraded, up to a certain point when resistivity increased precipitously (Figure 5.3a). This is believed to be aggravated by mechanical stylus patterning as it may damage the surface of the Mo layer to some degree. Surface damages will accelerate corrosion of the exposed Mo in the P3 scribe line as can be seen in Figure 5.3b. One way to avoid this issue completely would be to employ indirect induced laser patterning for the P3 isolation scribe, see Section 4.2.3.

Some results from these experiments that have so far remained unpublished are shown in Figure 5.2b. These results show a weakness in the state-of-the-art process flow of CIGS modules. We recall from the CIGS cell stack (Figure 1.5) that there is a thin resistive barrier layer (i-ZnO) and a thicker conducting top contact layer doped with aluminium (ZnO:Al). The purpose of the barrier layer is to protect modules (and cells) from potentially harmful shunt paths in the CIGS layer. By convenience, i.e. to be able to use one single vacuum step for both ZnO layers, P2 patterning is performed prior to deposition of both ZnO layers, see e.g. [81]. This in spite of some doubt expressed

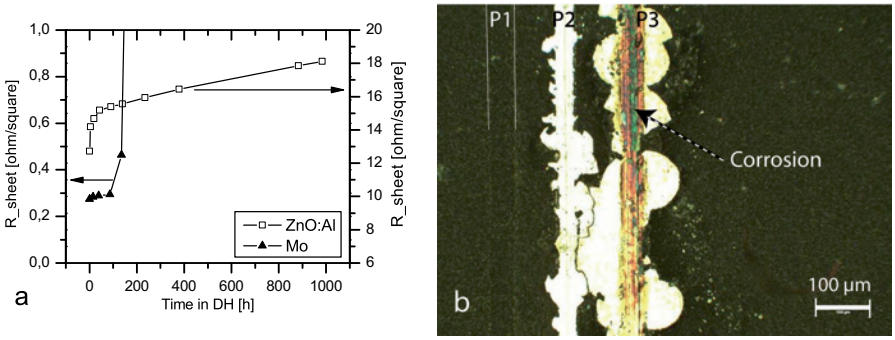

Figure 5.3: a) Bare contact layers deposited on glass exposed to damp heat. The Mo layer degraded rapidly by visual inspection but maintained a low sheet resistivity until completely destroyed at ≈150 h. b) Mo surface corrosion in P3 scribe line after 140 h in damp heat. Degradation appears more pronounced at the scribe line center where stylus damage may occur.

in CIGS research as the presence of the resistive layer also increases the resistive contribution of the P2 interconnect [64]. Our result shows a significant increase from 0.7 ohm·cm to 3.6 ohm·cm specific contact resistivity. And what is worse, when subject to damp heat testing test structures with i-ZnO in the interconnect degraded immediately to almost ten times that with a maximum of 27 ohm·cm (Figure 5.2b). That the degradation is immediate (only 4 hours into the test) suggests that a small amount of moisture may cause catastrophic degradation of conductivity. While laser P2 patterning approaches such as are described in Sections 4.2.1 and 4.3.1 are not likely to significantly change this relationship, it is possible that laser micro-welding (4.3.2) in the long term can decouple the i-ZnO layer from stability issues. However, as the current state of the micro-weld process results in mild to severe damage of the Mo and glass substrate long term stability is still not clear (see below).

5.2 Stability of laser patterned modules

5.2.1 Transformed CIGS P2 stability

In order for laser patterning to be a viable alternative to mechanical stylus patterning, the processes must not reduce the long term stability or performance of modules. In PAPER III we showed successful results when P2 patterning was performed by transformation of the CIGS to a conducting compound. Some stability testing was performed, showing stable output for 1000 h in dry heat (equivalent to assuming near perfect encapsulation) and for over a year in ambient conditions. These results are shown in Figure 5.4.

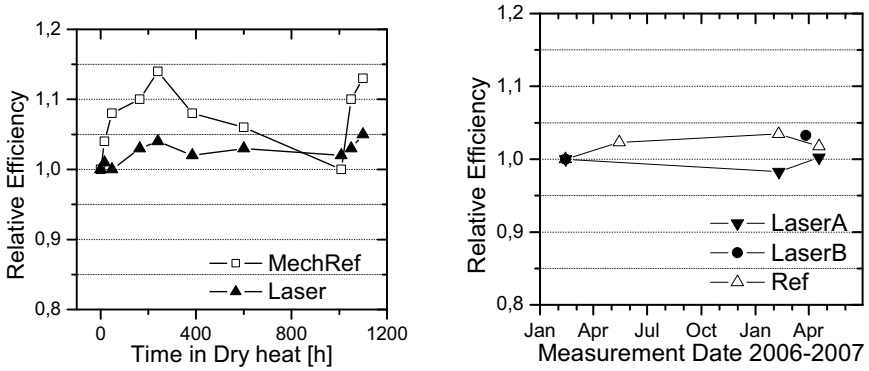

Figure 5.4: Stability of laser patterned modules was verified in a 1000 h heat test (left). Modules stored in ambient conditions maintained stable output for over a year (right).

5.2.2 Laser micro-weld P2 stability

The early experience indicates issues with stability. Degradation has been observed during ambient storage and dry heat testing, see PAPER VI. The degraded structures all suffered from the Mo layer damage and glass cracking that was introduced previously. With such poor integrity of the Mo layer it is highly likely corrosion will set on at an early stage. It is also possible that the glass cracking, which extended all the way through the cell stack, provided additional entry paths for ambient humidity into the various interfaces causing degradation. This hypothesis is strengthened by the fact that a sample processed at low laser power and with no apparent Mo or glass damages passed the dry heat stability test with power loss within 5 % of its initial value. These results are shown in Figure 5.5.

5.3 Reverse bias stability

In PAPER IV we investigated the effect of reverse bias stress on CIGS thin film modules and cells. Generally speaking, PV modules have a bypass diode in the junction box to protect them from being placed under conditions of reverse bias in case of string failure or faulty installation. Data has been reported suggesting that degradation of CIGS modules under reverse stress is completely reversible making bypass diodes unnecessary [82]. Even so, when shading of individual cells occurs in a module, that cell will operate under reverse bias conditions with the module voltage driving current through in the reverse direction.

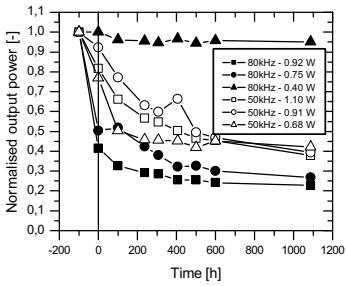

Figure 5.5: Dry heat stability test results for 6 of the micro-weld patterned modules plotted as output power change with time in dry heat normalised to as-deposited performance. Note that the as-deposited value is plotted for reference at -100 h for all samples although this is not the correct time frame. Time from initial measurement to test start ranged from 500 – 1500 h.

In our work we were able to use IR thermography to establish a connection between hot spots appearing during reverse stress and momentary increase in conductivity as well as visual defects ("worms"), see Figure 5.6. Monitoring the hot spot activity during reverse stress allowed us to disprove the assumption that they would appear primarily due to scribe line defects [83]. On the contrary, in both the module and cell samples we observed that a strong majority of hot spots originated in the cell bulk and moved toward the cell edge. We could also conclude that part of the performance degradation was reversible if stress had been applied along with illumination of the sample surface. Remaining losses were due to irreversible shunt paths created in the hot spot defects (see Figure 5.7). We believe that this permanent conductivity may be caused by resistive heating in the hot spot transforming the CIGS into a conducting compound. It would be similar to laser treated CIGS used as an electrical interconnection in CIGS modules, i.e. with segregation of Cu_xSe and Cu rich CIGS (Sections 4.3.1 and 4.3.2).

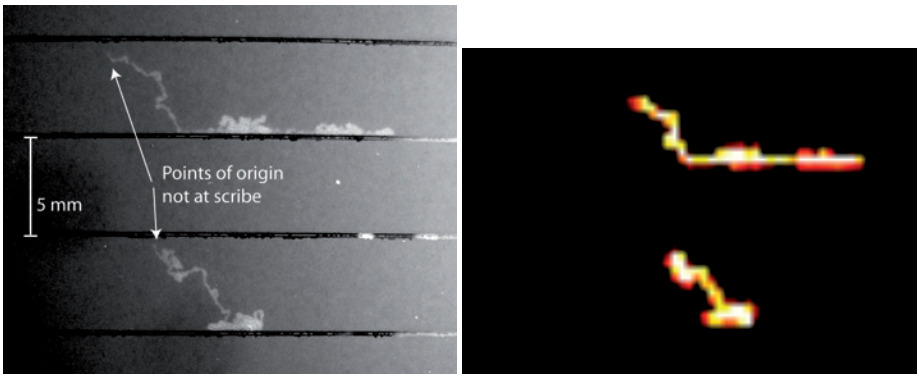

Figure 5.6: Wormlike defects on CIGS surface observed visually (left) and using IR thermography tracing (right).

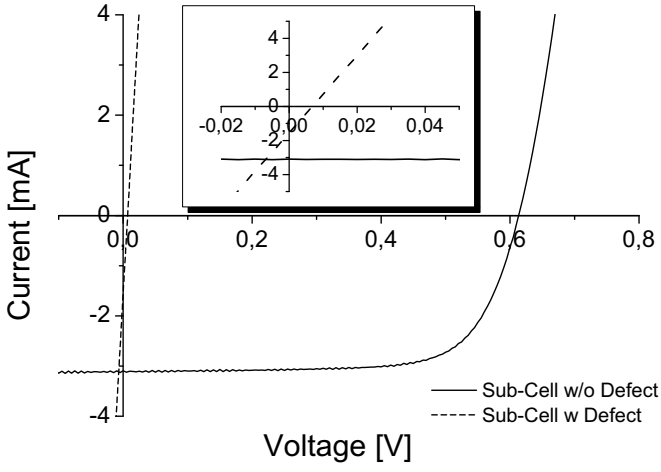

Figure 5.7: The visible defects correlated with complete shunting locally as showed by I-V measurement on sub-cells with and without visible defects.

6. Concluding remarks and outlook

Thin film photovoltaics as a large-scale, high throughput, industrial technology is, if not in its infancy, certainly still an adolescent with tricks to learn and challenges to meet. Development is fast and competitive as these so-called second generation solar cells are taking over larger and larger shares of the PV power generation market. If you trip up you may fall, but if you stand still you surely will be left behind.

In this thesis I have, through my experimental work and in cooperation with industry leading partners, attempted to test the possibilities of continued development in CIGS PV manufacturing, mainly through the use of laser patterning methods. Picosecond pulse durations is expected to be the next step in industrial laser development. With short laser-material interaction times they promise, and deliver, less thermal effects and more selective patterning options. In the thesis we have presented results showing the selective removal of ZnO:Al layer for top contact isolation in CIGS modules, known as P3 patterning. Removal of the top layer is achieved by ablating a very thin layer of the CIGS immediately underneath the ZnO:Al whereupon the top layer is removed explosively. This process is in itself ready for high-speed, high accuracy patterning as was highlighted by the very narrow (36 μm) ablation line width. It remains to be proven that laser system manufacturers can provide such systems that support 24/7 operation with little downtime or instabilities.

Using a more proven type of laser with nanosecond pulse duration I have been able to exploit the thermal nature of this laser-material interaction to transform CIGS into a conductive compound along a patterned line. This lead to the development of the *laser micro-welding* technique, for which we have filed an international patent application, whereby interconnective (P2) laser patterning can be performed after all layers have been deposited. Thermal action on the CIGS causes partial evaporation and results in an increased metallic ratio with segregation of Cu_xSe. This conductive "CIGS" works as the electrical connection between Mo bottom contact and ZnO:Al top contact. While the current process has proven difficult to control, with Mo and glass damage being the primary problems, we believe that the solution lies in beam shaping. Less power concentrated at the beam center and better power utilisation would avoid the detrimental damages. While the process still deserves further exploration, to determine whether the elimination of damage also eliminates the degradation observed for most samples, we have manufactured high per-

forming modules, the champion reaching 14.0 % efficiency with 71.5 % fill factor, and shown a successful proof of existence for stable behaviour.

Taken together, one can see that both P2 and P3 patterning can be performed after thin film deposition and junction formation, eliminating any contaminating debris or unnecessary exposure that might deteriorate cell quality. Implementing vacuum methods for buffer deposition, and with the design of a dual beam laser patterning tool, one could significantly reduce manufacturing times through reduced vacuum pumping, alignment and patterning steps.

Sammanfattning på Svenska

Solenergi och solceller

Energin i solljuset uppgår totalt i sådana mängder att två timmars solljus skulle räcka till att täcka det energibehov vår nuvarande civilisation har under ett år. Denna energi är fördelad i ett spektrum av energipaket, fotoner, från låga energier - vad vi kallar infraröd strålning - till höga energier där den kallas ultraviolett strålning. Det finns flest fotoner i den synliga delen av spektrumet, som ligger något lägre i energi än det ultravioletta ljuset. Strålningen sträcker sig långt ut i det infraröda området, men här finns inte mycket energi att hämta eftersom det är färre antal fotoner och dessutom vid lägre energier. Merparten av solljusets energi ligger mellan 1 - 4 elektronvolt (eV).

Solceller fungerar så att de kan omvandla fotonernas energi till elektrisk energi. Genom att materialet absorberar ljus ges dess elektroner en högre energi som kan utvinnas som en likström i en yttre krets mellan cellens (+) och (-) poler. Man kan säga att solcellens *ström* beror av antalet fotoner vars energi är högre än materialets inbyggda energi-steg. *Spänningen* för solcellen beror därefter framförallt av detta inbyggda energi-steg. Högre energi-steg leder alltså till högre spänning men även till färre fotoner som är tillgängliga och det gäller alltså att materialet tillfredställer denna kompromiss för att få en så hög uteffekt som möjligt. Vanligen har solcellsmaterial energi-steg mellan 1-2 eV.

CIGS är en förkortning av $CuIn_{1-x}Ga_xSe_2$ eller *koppar-indium-gallium-diselenid* och är ett av de mest lovande materialen för solceller baserade på tunnfilmsteknik med en laboratorieverkningsgrad på 20 %. Genom att använda sig av extremt tunna filmer ($\approx$0.005 mm) på ett bärande material (substrat) kan man spara på mängden material som behövs för effektiv utvinning av solenergi. Eftersom den dominerande kiseltekniken beror kraftigt av energiintensiva reningssteg sparar tunnfilmstekniken dessutom jämförelsevis på energi vid tillverkningen. En typisk tunnfilmspanel i södra Europa genererar lika mycket energi som använts vid tillverkning och installation under sitt första år. Med en förväntad livslängd på 25 år är resten en energivinst.

Tunnfilmssolceller ur ett tekniskt perspektiv

En tunnfilmssolcell av CIGS-typ består av 1) ett undre kontaktskikt av metall (molybden); 2) absorbatorlagret (CIGS) som tillsammans med 3) buffertskiktet av kadmiumsulfid utgör cellens funktionella kärna; 4) ett tunt resistivt skikt zinkoxid samt 5) ett tjockare, ledande zinkoxidskikt som tillsammans bildar en genomskinlig framkontakt. För att möjliggöra insamling av större mängder solenergi måste enskilda celler kopplas samman till en s.k. solcellsmodul eller solcellspanel. Att sammanföra celler genom tunnfilmsteknik kräver färre och enklare steg jämfört med den dominerande kiseltekniken där tunna skivor av kisel tillverkas individuellt, sorteras och sedan löds ihop. Även detta hjälper till att reducera produktionskostnader för tunnfilmspaneler gentemot kiseltekniken.

Genom att alternera beläggning och mönstring av tunna filmer åstadkommer man både isolering och seriekoppling av intilliggande celler. Denna sammankoppling ingår därefter i lagrens egen struktur. Detta kallas för monolitisk (i ett stycke el. egentligen "i en sten") integrering och avlägsnar behovet att i efterhand sammankoppla celler. Mönstringen leder till vissa förluster, framförallt förlorad yta som istället upptas av kontakterna samt elektriska resistenser. Ju smalare mönsterlinjer och ju närmare varandra de kan placeras desto mer aktiv yta finns tillgänglig för generering av elektricitet. För smala kontakter skulle dock kunna leda till höga resistenser i kontakten eller kortslutningar mellan celler.

Med hjälp av laserteknik kan man åstadkomma smalare linjer än genom att använda nålar av metall för att mönstra halvledarskikten. Detta innebär en ökning av den aktiva solcellsarean och därigenom högre verkningsgrad på modulnivå. En minskning från 350 μm till 150 μm förlorad bredd skulle innebära strax över 4 % mer ström i modulen. Lasertekniken är kompatibel med höga hastigheter och god precision för mönstring. Det finns även vissa utmaningar när laser skall användas, framförallt hur man skall mönstra vissa enskilda skikt utan att skada andra. Lasermönstring sker genom att lokalt smälta och/eller förånga material på en väldigt kort tid (10^{-13} - 10^{-8} s) vilket leder till att detta material avlägsnas. Genom att utnyttja laserns möjlighet att passera igenom transparenta material, exempelvis glas som är det vanliga bärande lagret för tunnfilmssolceller, kan man även åstadkomma en explosiv expansion i en films undersida och därigenom avlägsna det vid lägre lasereffekt eftersom endast en liten del av materialet behöver förångas. Resten sprängs bort av expansionens kraft i form av damm. Eftersom lasermönstringen sker genom att energi tillförs skikten lokalt sker ofta värmeledning till omkringliggande områden varpå skador kan ske längs linjens kant eller på intilliggande skikt. Ju kortare laserpulser man tillämpar, desto mindre blir dessa värmeeffekter.

I detta arbete har vi fokuserat på hur lasermönstring kan användas inom monolitisk integrering av tunnfilmssolceller av CIGS-typ. Vi har konstaterat att lasermönstring inte lider av de ojämna flagor som uppstår vid mekanisk

ritsning och därmed upptar lasermönstrade linjer en mindre del av solpanelens yta vilket ökar dess totala verkningsgrad.

Vi har kunnat konstatera att CIGS, som är en halvledare, kan genom laserbehandling omvandlas till en lokalt ledande "sträng" som ersätter den direkta kontakten mellan övre och undre kontaktskikt. Ledningsförmågan förklaras av att CIGS-materialet undergår partiell förångning av framförallt indium och selen, men även gallium vilket leder till en kopparrik sammansättning. Kopparrik CIGS uppvisar ofta en hög ledningsförmåga och det förutsätts att även den ledande föreningen koppar-selenid segregerar och bidrar till en ökad ledningsförmåga. Under arbetet har högpresterande minimoduler producerats med verkningsgrad upp till 15 % trots att den uppmätta längdspecifika[1] kontaktresistansen varit något högre än för mekaniskt mönstrade kontakter, 0.4 ohm·cm jämfört med 0.1 ohm·cm respektivt. Denna ökning kan verka relativt hög men motsvaras av ett spänningsfall på 6 mV respektive 1.5 mV vid standardinstrålning då cellspänningen är ca 530 mV och förlusten är alltså endast någon procent.

Denna typ av ledande "CIGS" har vi även visat att det är möjligt att producera med en teknik vi valt att kalla *laser mikrosvetsning*. Enligt denna teknik kan man belägga alla halvledarskikt i följd, utan avbrott för mönstring. Ur industriellt perspektiv kan man se tids- och energivinster genom att en sekvens av vakuumprocesser kan utföras i en följd, utan att bryta vakuumet. Dessutom kan man förvänta sig att detta i sin tur ger förbättrad kontroll av gränsskikten med högre cellkvalitet som följd. Själva mönstringssteget utförs alltså efter att alla skikt är på plats. Lasern transformerar CIGS-skiktet samtidigt som en kontakt till det övre kontaktskiktet skapas genom att materialet fördelas om något på grund av krafterna som verkar på det smälta materialet. Vi har kunnat visa på utomordentliga prestanda både i jämförelse med mekaniskt ritsade referenser och med ett toppresultat med en verkningsgrad på 14.0 %. Processen har skalats upp till 30x30 cm^2 substratstorlek för att visa på dess potential för industriellt användande. Dock har flera utmaningar med denna process identifierats där det främst handlar om skador på det underliggande kontaktskiktet av molybden som uppvisat kraftiga sprickor och avbrott. Även glasskador har observerats som konsekvens av värmeutvidgning i den glassubstratet. Vi föreslår att en förändrad fördelning av energin i laserstrålen, där effekten fördelas jämnt över ytan - s.k. "top hat" -, skulle kunna bidra starkt till förbättrad kontroll och ett större processfönster.

Vi har dessutom visat hur man genom att använda pikosekundsnabba laserpulser kan avlägsna den övre kontakten selektivt genom att utnyttja den höga absorptionen i CIGS skiktet. Genom att förånga endast en bråkdel av CIGS lagret vid gränsskiktet sprängs zinkoxidskiktet bort på ett kontrollerat sätt. Den snabba interaktionen minimerar värmeledning och termiska effekter under

[1] Den totala resistansen beror av cellens längd och minskar ju längre cellen är.

mönstringen och därigenom undviks signifikant påverkan på CIGS-skiktets ledningsförmåga och isolation mellan intilliggande celler uppnås.

Sammantaget skulle man alltså kunna göra de två mönstringsstegen P2 och P3 med laserprocesser. Genom att designa ett kombinerat mönstringssystem skulle mönstringen kunna ske samtidigt och efter det att själva cellstrukturen formats. Simultan mönstring skulle ytterligare minska processtiden för CIGS-moduler då ett enda linjerings- och mönstringssteg skulle ersätta två.

Slutligen har inkapsling och stabilitet behandlats. Tunnfilmsteknik är generellt känsligare för degradationer och yttre påverkan just eftersom det rör sig om ytterst tunna skikt. För kvalifikation och utveckling utsätter man därför paneler för en rad tester för att identifiera och därigenom kunna förbättra eventuella svagheter. Ett av de mest påfrestande testen för CIGS-teknik har visat sig vara klimattest under hög värme och fuktighet (85 °C och 85 % relativ fuktighet) under 1000 timmar. Vår forskning har visat att fukt är av avgörande betydelse för försämrad modulprestanda och att om en fuktbarriär används vid inkapsling av modulerna klarar de av detta test. Tester av oinkapslade moduler har visat på svagheter som beror av mönstringsteknik, nämligen ytskador i molybdenskiktet och försämrade kontakter då mönstringen sker innan beläggning av det s.k. resistiva zinkoxidskiktet. Med hjälp av den lasermönstringsteknik som skulle ersätta mekanisk P3 skulle dessa ytskador undvikas. Stabiliteten hos lasermönstrade moduler har utvärderats under torra förhållanden, således förutsatt en nära nog perfekt inkapslingsteknik, och dessa tester har visat på önskad stabilitet samtidigt som de skador som identifierats för mikrosvetsade kontakter satts i samband med kraftig degradation redan innan testet kunnat utföras.

Lasertekniken utvecklas snabbt framåt och kommer med all sannolikhet inom kort att ha ersatt de mekaniska metoder som nu används för att mönstra solcellsmoduler av CIGS-typ. För att detta ska ske krävs att system med pikosekundlaser blir stabilare och mer ekonomiska. Mikrosvetsning är en ytterst intressant metod som skulle innebära dramatiska vinster i tillverkningstider och energiåtgång för CIGS-moduler, men det kvarstår att genom teknisk utveckling bredda arbetsområdet där stabila och väl fungerande kontakter kan tillverkas.

Acknowledgements

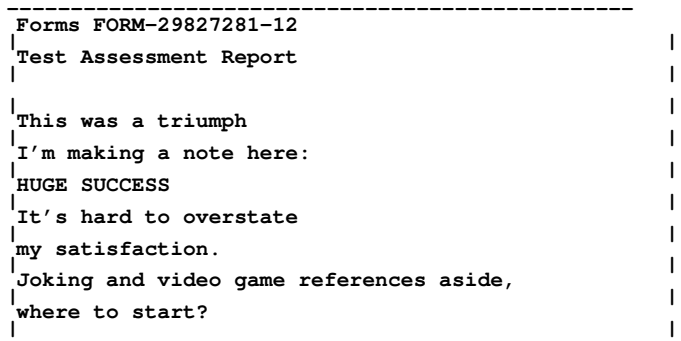

My son, for coming into our life just when this work was beginning to boil down and keeping my mind off thesis writing at least a few hours per day. My lovely, beautiful, and far-too-good-for-me fiancée for support, understanding and love. You two are not part of my life - you are my life.

Uwe, for part time supervision and full time inspiration. If I am ever half of what you are I will be brilliant. Marika, for always - always - having an optimistic spirit, five minutes and a smile in store. Even during the more stressful times. Your support has been a great strength to draw from when needed. To Lars for believing in my work and taking me on as the first industrial PhD student at Solibro Research. All the Ångström Solar Center PhD students, past and present, for constant camaradery and support. I must mention some of the crackling sparks that shot off the embers of academia ahead of me. Jonas whose PhD defence was my first glimpse at the future. Adam who had the audacity to start after me and finish before me. Thanks for a great time of office sharing and offering all the jokes and distraction I could have wanted (and more). Lotten for your inspiring dedication. Ulf whose cool quiet grace extended through to the end. Jens - you are missed! Hope you graduate this year. Sebastian, Jonas, Timo, Pjotr, Johan, Tove... best of luck! Writing a thesis is actually kind of fun. For now, just focus on enjoying this opportunity and getting results (and keeping the results organized). Tobias, good luck with the important progress. Jon, thanks for all the donuts.

Of course, the entire division of Solid State Electronics deserves recognition for the supportive social and professional environment. Particularly Lina, for a capacity of turning sighs into laughter, and who always makes me realise I have no problems at all. Jörgen, for some good insights on my first draft. Marianne for holding this ship together and making sure there is never a shortage of fika or coffee. Hanna Yousef (I know, different division..) for tricking me into joining the Departmental Board and for having such a smiling spirit.

Thanks also to the entire Solibro Research team (who has grown so fast I will mention no names to avoid leaving any out) for providing me with material and helping me destroy it. I mean test it.

A big, warm thanks to my parents, brothers and extended family in all directions. I never doubted the irrelevance of my academic success in your company, ever fonder as it is.

To the Book club. New and old friends. I bet you loved this book, but please let me skip the meeting when we discuss it.

I began this thesis with a quote and I will end it with a different one, from a man who did what I contemplated many a time over these past ten years.

He dropped out and became a rock star.

"I guess this is my dissertation
*Homie, this sh*t is basic*
Welcome to Graduation"
- Kanye West

```
|                                                  |
|There's no sense crying over every mistake        |
|                                                  |
|you just keep on trying til you run out of cake   |
|                                                  |
|and then the Science gets done.                   |
|                                                  |
|                                                  |
|--------------------------------------------------|
```

Bibliography

[1] V. Smil. *Energy - a beginner's guide*. Oneworld Publications, Oxford, 2006.

[2] BP Statistical Review of World Energy June 2010. Statistical report, 2010-12-20 2010.

[3] C. Kittel. *Introduction to Solid State Physics*. John Wiley and sons, Inc., New York, 7th edition, 1996.

[4] M. A. Green. *Solar Cells - Operating Principles, Technology and System Applications*. The University of New South Wales, 1998.

[5] E. A. Alsema and E. Nieuwlaar. Energy viability of photovoltaic systems. *Energy Policy*, 28(14):999–1010, 2000.

[6] M. A. Green, K. Emery, Y. Hishikawa, and W. Warta. Solar cell efficiency tables (version 36). *Progress in Photovoltaics: Research and Applications*, 18(5):346–52, 2010.

[7] A. J. Breeze. Next generation thin-film solar cells. 2008 IEEE International Reliability Physics Symposium (IRPS), pages 168–71, Piscataway, NJ, USA, 2008. IEEE.

[8] S. Niki, M. Contreras, I. Repins, M. Powalla, K. Kushiya, S. Ishizuka, and K. Matsubara. CIGS absorbers and processes. *Progress in Photovoltaics: Research and Applications*, 18(6):453–466.

[9] E. A. Alsema, M. J. de Wild-Scholten, and V. M. Fthenakis. Environmental impacts of PV electricity generation - A critical comparison of energy supply options. In *21st European Photovoltaic Solar Energy Conference*, Dreseden, Germany, 2006. WIP-Renewable Energies.

[10] V. M. Fthenakis and H. C. Kim. Photovoltaics: Life-cycle analyses. *Solar Energy*, In Press, Corrected Proof, 2010.

[11] International Energy Agency Report - Key World Energy Statistics 2010. Technical report, Published in October 2010.

[12] N. G. Dhere. Toward GW/year of CIGS production within the next decade. *Solar energy materials and solar cells*, 91(15-16):1376–82, 2007.

[13] G. Watt and H. Fechner. Photovoltaic market and industry trends - latest results from the IEA PVPS programme. *Elektrotechnik und Informationstechnik*, 126(9):328–330, 2009.

[14] Press Release: Q-Cells sets a new 13.0 % efficiency record for mass-produced CIGS thin-film modules, 2009.
http://www.solibro-solar.com/en/company/investor_relations/ corporate_news/ 09062010_qcells_sets_a_new_130 _efficiency_record_ for_massproduced_cigs_thinfilm _modules/index.html
available online 2011-01-18.

[15] MiaSolé - Company Website, 2011. www.miasole.com.

[16] Global Solar Energy - Company Website, 2011. www.globalsolar.com.

[17] Odersun AG - Company website, 2011. www.odersun.com.

[18] M. Winkler, J. Griesche, I. Konovalov, J. Penndorf, J. Wienke, and O. Tober. CISCuT - solar cells and modules on the basis of CuInS2on Cu-tape. *Solar Energy*, 77(6):705–16, 2004.

[19] J. S. Britt, E. Kanto, S. Lundberg, and M. E. Beck. CIGS device stability on flexible substrates. volume 1 of *Conference Record of the 2006 IEEE 4th World Conference on Photovoltaic Energy Conversion, WCPEC-4*, pages 352–355, Waikoloa, HI, United states, 2007. Inst. of Elec. and Elec. Eng. Computer Society.

[20] U. Zimmermann, M. Ruth, and M. Edoff. Cadmium-free CIGS mini-modules with ALD-grown Zn(O,S)-based buffer layers. In *21st European Photovoltaic Solar Energy Conference*, pages 1831–1834, Dresden, 2006. WIP-Renewable Energies.

[21] F. Kessler and D. Rudmann. Technological aspects of flexible CIGS solar cells and modules. *Solar Energy*, 77(6):685–695, 2004.

[22] C. Dunsky and F. Colville. Solid state laser applications in photovoltaics manufacturing. volume 6871 of *Proc. SPIE - Int. Soc. Opt. Eng. (USA)*, pages 687129–1, USA, 2008. SPIE - The International Society for Optical Engineering.

[23] P. M. Harrison and S. Ellwi. Industrial applications of high-average power high-peak power nanosecond pulse duration Nd:YAG lasers. volume 7193 of *Proc. SPIE - Int. Soc. Opt. Eng. (USA)*, page 71932A (9 pp.), USA, 2009. SPIE - The International Society for Optical Engineering.

[24] H. P. Huber, F. Herrnberger, S. Kery, and S. Zoppel. Selective structuring of thin-film solar cells by ultrafast laser ablation. In *Commercial and Biomedical Applications of Ultrafast Lasers VIII*, volume 6881 of *Proceedings of SPIE - The International Society for Optical Engineering*, pages Society of Photo–Optical Instrumentation Engineers (SPIE), San Jose, CA, United states, 2008. SPIE.

[25] G. Eberhardt, H. Banse, U. Wagner, and T. Peschel. Structuring of thin film solar cells. volume 7585 of *Proc. SPIE - Int. Soc. Opt. Eng. (USA)*, page 75850P (10 pp.), USA, 2010. SPIE - The International Society for Optical Engineering.

[26] H. P. Huber, M. Englmaier, C. Hellwig, A. Heiss, T. Kuznicki, M. Kemnitzer, H. Vogt, R. Brenning, and J. Palm. High speed structuring of CIS thin-film solar cells with picosecond laser ablation. volume 7203 of *Proc. SPIE - Int. Soc. Opt. Eng. (USA)*, page 72030R (9 pp.), USA, 2009. SPIE - The International Society for Optical Engineering.

[27] J. Bonse, R. Patel, S. Maneuf, R. Desailly, C. Devasia, and D. Clark. Recent advances in laser scribing process technologies for thin film solar cell manufacturing. In *23rd European Photovoltaic Solar Energy Conference*, pages 2325–2327, Valcencia, Spain, 2008. WIP-Renewable Energies.

[28] W. M. Steen. *Laser Material Processing*. Springer-Verlag, London, 2nd edition, 1998.

[29] S. M. Metev and V. P. Veiko. *Laser-Assisted Micro-Technology*, volume 19 of *Materials Science*. Springer-Verlag, Berlin, 2nd edition, 1998.

[30] P. W. Milonni and J. H. Eberly. *LASERS*. John Wiley and sons, New York, 1st edition, 1988.

[31] M. C. Gower. Industrial applications of laser micromachining. *Optics Express*, 7(2), 2000.

[32] D. Hauschild, O. Homburg, T. Mitra, M. Ivanenko, M. Jarczynski, J. Meinschien, A. Bayer, and V. Lissotschenko. Optimizing laser beam profiles using micro-lens arrays for efficient material processing: Applications to solar cells. volume 7202 of *Proc. SPIE - Int. Soc. Opt. Eng. (USA)*, page 72020U (15 pp.), USA, 2009. SPIE - The International Society for Optical Engineering.

[33] D. Keming. Thin layer ablation with lasers of different beam profiles - energy efficiency and over filling factor. volume 7202 of *Proc. SPIE - Int. Soc. Opt. Eng. (USA)*, page 72020Q (9 pp.), USA, 2009. SPIE - The International Society for Optical Engineering.

[34] G. Heise, C. Hellwig, T. Kuznicki, S. Sarrach, C. Menhard, A. Heiss, H. Vogt, J. Palm, and H. P. Huber. Monolithic interconnection of CIGSSe solar cells by picosecond laser structuring. volume 7585 of *Proc. SPIE - Int. Soc. Opt. Eng. (USA)*, page 75850U (12 pp.), USA, 2010. SPIE - The International Society for Optical Engineering.

[35] J. Hermann, M. Benfarah, S. Bruneau, E. Axente, G. Coustillier, T. Itina, J. F. Guillemoles, and P. Alloncle. Comparative investigation of solar cell thin film processing using nanosecond and femtosecond lasers. *Journal of Physics D: Applied Physics*, 39(3):453–460, 2006.

[36] S. T. Davies, E. C. Harvey, H. Jin, J. P. Hayes, M. K. Ghantasala, I. Roch, and L. Buchaillot. Characterization of micromachining processes during KrF excimer laser ablation of TiNi shape memory alloy thin sheets and films. *Smart Materials and Structures*, 11(5):708–714, 2002.

[37] D. Bäuerle. *Laser processing and chemistry*. Springer, Berlin, Heidelberg, New York, 3 edition, 2000.

[38] J. Bovatsek, A. Tamhankar, R. S. Patel, N. M. Bulgakova, and J. Bonse. Thin film removal mechanisms in ns-laser processing of photovoltaic materials. *Thin Solid Films*, 518(10):2897–2904, 2010.

[39] A. Fell, S. Hopman, D. Kray, and G. P. Willeke. Transient 3D-simulation of laser-induced ablation of silicon. In *22nd European Photovoltaic Solar Energy Conference*, Milan, Italy, 2007. WIP-Renewable Energies.

[40] M. Colina, C. Molpeceres, M. Morales, F. Allens-Perkins, G. Guadaño, and J. L. Ocaña. Modelling of laser ablation processes for applications in thin film photovoltaic technology. In *23rd European Photovoltaic Solar Energy Conference*, Valencia, 2008. WIP-Renewable Energies.

[41] T.-W. Kim, H.-J. Pahk, H. K. Park, D. J. Hwang, and C. P. Grigoropoulos. Comparison of multilayer laser scribing of thin film solar cells with femto, pico and nanosecond pulse durations. volume 7409 of *Proceedings of SPIE - The International Society for Optical Engineering*, page The International Society for Optical Engineering (SPIE), San Diego, CA, United states, 2009. SPIE.

[42] E. Schneiderlochner, A. Grohe, S. W. Glunz, R. Preu, and W. Willeke. Scanning Nd:YAG laser system for industrially applicable processing in silicon solar cell manufacturing. volume Vol.2 of *Proceedings of 3rd World Conference on Photovoltaic Energy Conversion (IEEE Cat. No.03CH37497)*, pages 1364–7, Japan, Japan, 2003. Arisumi Printing Inc.

[43] R. Mayerhofer, L. llers, and A. Becker. Laser micro-processing in solar cell production. volume 1 of *Conference Record of the 2006 IEEE 4th World Conference on Photovoltaic Energy Conversion, WCPEC-4*, pages 1115–1118, Waikoloa, HI, United states, 2007. Inst. of Elec. and Elec. Eng. Computer Society.

[44] H. Schmidhuber, S. Klappert, J. Stollhof, G. Erfurt, M. Eberspächer, and R. Preu. Laser Soldering - A technology for better contacts. In *20th European Photovoltaic Solar Energy Conference*, Bacelona, 2005. WIP-Renewable Energies.

[45] T. Rublack, M. Alemán, and S. W. Glunz. Evaluation of the laser melting process of different materials for the front-side metallization of silicon solar cells. In *23rd European Photovoltaic Solar Energy Conference*, Valencia, Spain, 2008. WIP-Renewable Energies.

[46] P. Engelhart. Laser processing for high efficiency silicon solar cells. volume 7202 of *Proceedings of SPIE - The International Society for Optical Engineering*, page The International Society for Optical Engineering (SPIE), San Jose, CA, United states, 2009. SPIE.

[47] H. J. Booth. Recent applications of pulsed lasers in advanced materials processing. *DOPS-NYT*, 20(2):33–6, 2005.

[48] M. Abbott and J. Cotter. Optical and electrical properties of laser texturing for high-efficiency solar cells. *Progress in Photovoltaics: Research and Applications*, 14(3):225–235, 2006.

[49] A. G. Aberle. Fabrication and characterisation of crystalline silicon thin-film materials for solar cells. *Thin Solid Films*, 511-512:26–34, 2006.

[50] S. Beyer, V. Tornari, and D. Gornicki. Comparison of laser induced front- and rear-side ablation. volume 5063 of *Proc. SPIE - Int. Soc. Opt. Eng. (USA)*, pages 202–7, USA, 2003. SPIE-Int. Soc. Opt. Eng.

[51] S. Wiedeman, M. E. Beck, R. Butcher, I. Repins, N. Gomez, B. Joshi, R. G. Wendt, and J. S. Britt. CIGS module development on flexible substrates. Conference Record of the Twenty-Ninth IEEE Photovoltaic Specialists Conference 2002 (Cat. No.02CH37361), pages 575–8, Piscataway, NJ, USA, 2002. IEEE.

[52] F. Kessler, D. Herrmann, and M. Powalla. Approaches to flexible CIGS thin-film solar cells. *Thin Solid Films*, 480-481:491–498, 2005.

[53] P. Gečys, G. Račiukaitis, M. Ehrhardt, K. Zimmer, and M. Gedvilas. ps-laser scribing of CIGS films at different wavelengths. *Applied Physics A: Materials Science & Processing*, pages 1–6, 2010.

[54] P. Gečys, G. Račiukaitis, M. Gedvilas, and A. Selskis. Laser structuring of thin-film solar cells on polymers. *EPJ Applied Physics*, 46(1):12508p1–12508p6, 2009.

[55] P. O. Westin. *Optimisation of laser scribing of back contact for photovoltaic modules*. MSc Thesis, Luleå University of Technology, 2005.

[56] A. G. Aberle. Thin-film solar cells. *Thin Solid Films*, 517(17):4706–10, 2009.

[57] S. Avagliano, N. Bianco, O. Manca, and V. Naso. Combined thermal and optical analysis of laser back-scribing for amorphous-silicon photovoltaic cells processing. *International Journal of Heat and Mass Transfer*, 42(4):645–56, 1999.

[58] S. Haas, S. Ku, G. Schöpe, K. Du, U. Rau, and H. Stiebig. Patterning of thin-film silicon modules using lasers with tailored beam shapes and different wavelengths. In *23rd European Photovoltaic Solar Energy Conference*, pages 2383–2387, Valencia, 2008. WIP-Renewable Energies.

[59] J. Su, D. Tanner, and C. Eberspacher. Large Scale Thin Film Photovoltaic Laser Scribing Process. In *23rd European Photovoltaic Solar Energy Conference*, Valencia, 2008. WIP-Renewable Energies.

[60] J. Zhang, L. Feng, Z. Lei, Y. Cai, W. Li, L. Wu, B. Li, W. Cai, and J. Zheng. Preparation and performance of thin film CdTe mini-module. *Solar energy materials and solar cells*, 93(6-7):966–9, 2009.

[61] A. D. Compaan, I. Matulionis, and S. Nakade. Laser scribing of polycrystalline thin films. *Optics and Lasers in Engineering*, 34(1):15–45, 2000.

[62] D. Ruthe, K. Zimmer, and T. Hoche. Etching of $CuInSe_2$ thin films - Comparison of femtosecond and picosecond laser ablation. *Applied Surface Science*, 247(1-4):447–452, 2005.

[63] A. Buzas and Z. Geretovszky. Patterning ZnO layers with frequency doubled and quadrupled Nd:YAG laser for PV application. *Thin Solid Films*, 515(24 SPEC ISS):8495–8499, 2007.

[64] A. E. Delahoy and L. Chen. Advanced CIGS Photovoltaic Technology: Annual Technical Report, 15 November 2001-14 November 2002. Technical Report NREL/SR-520-33836, 01 May 2003.

[65] J. Hermann, M. Benfarah, G. Coustillier, S. Bruneau, E. Axente, J. F. Guillemoles, M. Sentis, P. Alloncle, and T. Itina. Selective ablation of thin films with short and ultrashort laser pulses. *Applied Surface Science*, 252(13 SPEC ISS):4814–4818, 2006.

[66] H. P. Huber, M. Englmaier, C. Hellwig, G. Heise, M. Kemnitzer, T. Kuznicki, C. Menhard, R. Brenning, A. Heiss, H. Vogt, and J. Palm. Picosecond laser structuring for the monolithic serial interconnection of CIS solar cells. In *24th European Photovoltaic Solar Energy Conference*, Hamburg, 2009. WIP-Renewable Energies.

[67] S. Wiedeman, R. Butcher, J. Fogleboch, J. Muha, R. G. Wendt, M. E. Beck, and J. S. Britt. CIGS processing on flexible polyimide substrates. In *National Center for Photovoltaics Program Review Meeting*, pages 49–50, Colorado, 2001.

[68] J. Kessler, S. Wiedeman, L. Russell, J. Fogleboch, S. Skibo, R. Arya, and D. Carlson. $Cu(In,Ga)Se_2$ based submodule process robustness. In *25th IEEE PVSC*, Conference Record of the IEEE Photovoltaic Specialists Conference, pages 813–816, Washington, DC, USA, 1996. IEEE, Piscataway, NJ, USA.

[69] A. Hultquist. *Cadmium Free Buffer Layers and the Influence of their Material Properties on the Performance of* $Cu(In,Ga)Se_2$ *Solar Cells*. Doctoral, Uppsala University, 2010.

[70] P. Jackson, R. Wurz, U. Rau, J. Mattheis, M. Kurth, T. Schlotzer, G. Bilger, and J. H. Werner. High quality baseline for high efficiency $Cu(In_{1-x},Ga_x)Se_2$ solar cells. *Progress in Photovoltaics: Research and Applications*, 15(6):507–519, 2007.

[71] Sunpower - Company website, 2011. http://us.sunpowercorp.com/.

[72] Suntech - Company website, 2011. http://www.suntech-power.com/.

[73] J. A. del Cueto, S. Rummel, B. Kroposki, and A. Anderberg. Long-term performance data and analysis of CIS/CIGS modules deployed outdoors. volume 7045 of *Proc. SPIE - Int. Soc. Opt. Eng. (USA)*, page 704504 (11 pp.), USA, 2008. SPIE - The International Society for Optical Engineering.

[74] IEC 61646: Thin-film terrestrial photovoltaic (PV) modules, Accessed 2010-12-20. Design qualification and type approval (available from www.iecee.org).

[75] C. R. Osterwald and T. J. McMahon. History of accelerated and qualification testing of terrestrial photovoltaic modules: a literature review. *Progress in Photovoltaics: Research and Applications*, 17(1):11–33, 2009.

[76] J. Wennerberg, J. Kessler, M. Bodegård, and L. Stolt. Damp heat testing of high performance CIGS thin film solar cells. In *2nd World Conference on Photovoltaic Solar Energy Conversion*, pages 1161–1164, 1998.

[77] U. Malm and L. Stolt. Long Term Stability ni Cu(In,Ga)Se2 Solar Cells with Different Buffer Materials. In *20th European Photovoltaic Solar Energy Conference*, Barcelona, 2005. WIP-Renewable Energies.

[78] U. Malm, M. Edoff, and L. Stolt. The Stability in Damp Heat Conditions of Thin-Film CIGS Solar Cells with Different Absorber Thicknesses. In *19th European Photovoltaic Solar Energy Conference*, Paris, 2004. WIP-Renewable Energies.

[79] J. Malmström, J. Wennerberg, and L. Stolt. A study of the influence of the Ga content on the long-term stability of Cu(In,Ga)Se2 thin film solar cells. *Thin Solid Films*, 431-432:436–442, 2003.

[80] J. Wennerberg, J. Kessler, and L. Stolt. Design of grided $Cu(In,Ga)Se_2$ thin-film PV modules. volume 67 of *Sol. Energy Mater. Sol. Cells (Netherlands)*, pages 59–65, Netherlands, 2001. Elsevier.

[81] J. Palm, V. Probst, and F. H. Karg. Second generation CIS solar modules. *Solar Energy*, 77(6):757–765, 2004.

[82] C. Köble, J. Klaer, R. Klenk, and M. C. Lux-Steiner. Stability of $CuInS_2$ Module Test Structures under Reverse Bias Stress. In *21st European Photovoltaic Solar Energy Conference, 4-8 September*, page 3, Dresden, Germany, 2006.

[83] E. E. v. Dyk, C. Radue, and A. R. Gxasheka. Characterization of $Cu(In,Ga)Se_2$ photovoltaic modules. *Thin Solid Films*, 515(15 SPEC ISS):6196–6199, 2007.

Acta Universitatis Upsaliensis

Digital Comprehensive Summaries of Uppsala Dissertations from the Faculty of Science and Technology 731

Editor: The Dean of the Faculty of Science and Technology

A doctoral dissertation from the Faculty of Science and Technology, Uppsala University, is usually a summary of a number of papers. A few copies of the complete dissertation are kept at major Swedish research libraries, while the summary alone is distributed internationally through the series Digital Comprehensive Summaries of Uppsala Dissertations from the Faculty of Science and Technology. (Prior to January, 2005, the series was published under the title "Comprehensive Summaries of Uppsala Dissertations from the Faculty of Science and Technology".)

Distribution: publications.uu.se
urn:nbn:se:uu:diva-143154

ACTA
UNIVERSITATIS
UPSALIENSIS
UPPSALA
2011